



HAL
open science

Analysis of two active set type methods to solve unilateral contact problems

Stéphane Abide, Mikaël Barboteu, David Danan

► **To cite this version:**

Stéphane Abide, Mikaël Barboteu, David Danan. Analysis of two active set type methods to solve unilateral contact problems. *Computational & Applied Mathematics*, 2016, 284, pp.286-307. 10.1016/j.amc.2016.03.012 . hal-01370169

HAL Id: hal-01370169

<https://hal.science/hal-01370169>

Submitted on 31 Jan 2023

HAL is a multi-disciplinary open access archive for the deposit and dissemination of scientific research documents, whether they are published or not. The documents may come from teaching and research institutions in France or abroad, or from public or private research centers.

L'archive ouverte pluridisciplinaire **HAL**, est destinée au dépôt et à la diffusion de documents scientifiques de niveau recherche, publiés ou non, émanant des établissements d'enseignement et de recherche français ou étrangers, des laboratoires publics ou privés.

Analysis of two active set type methods to solve unilateral contact problems

Stéphane Abide, Mikaël Barboteu¹ and David Danan

stephane.abide@univ-perp.fr, barboteu@univ-perp.fr, david.danan@univ-perp.fr

*Laboratoire de Mathématiques et Physique
Université de Perpignan Via Domitia
52 Avenue Paul Alduy, 66860 Perpignan, France*

Abstract

In this work two active set type methods are considered in order to solve a mathematical problem which describes the frictionless contact between a deformable body and a perfectly rigid obstacle, the so-called Signorini Problem. These methods are the primal dual active set method and the projection iterative method. Our aim, here, is to analyse these two active set type methods and to carry out a comparison with the well-known augmented Lagrangian method by considering two representative contact problems in the case of large and small deformation. After presenting the mechanical formulation in the hyperelasticity framework, we establish weak formulations of the problem and the existence result of the weak solution is recalled. Then, we give the finite element approximation of the problem and a description of the numerical methods is presented. The main result of this work is to provide a convergence result for the projection iterative method. Finally, we present numerical simulations which illustrate the behavior of the solution and allow the comparison of the numerical methods.

AMS Subject Classification: 74M15, 74G15, 74B05, 74B20, 74S30, 49M15, 90C53, 90C25, 65K15

Key words: Unilateral constraint, Hertzian contact, Hyperelasticity, Fixed point equation, Weak solution, Finite element approximation, Projection iterative method, Primal dual Active set, Augmented Lagrangian, Numerical simulations, Error estimates.

¹Corresponding author.

1. Introduction

Various contact boundary conditions have been used to model contact phenomena, both in engineering and mathematics in the literature; see for instance [10, 11, 24, 25, 27] and the references therein for the mathematical analysis and [12, 17, 20, 21, 28] for the numerical analysis. One of the most popular remains the so-called Signorini condition, introduced in [26], which describes the contact with a perfectly rigid foundation. Expressed in terms of unilateral constraints for the displacement field, this condition leads to a nonlinear and nonsmooth mathematical problem. To overcome these difficulties, several methods were used. For instance, Alart and Curnier presented in [1] an augmented Lagrangian formulation combined with a Generalized Newton method to solve non differentiable but continuous equations arising from frictional contact problems. Over the last few years, several other methods emerged. Amongst them, the active set strategies have been relatively popular for the last decade or so. The aim of this kind of method is to find the correct subset \mathcal{A} of all nodes that are currently in contact with the perfectly rigid obstacle; those nodes are called active while the others are inactive, see [16, 18] and references therein for more details. Also, one of the most interesting aspects of such a method is that it does not require the use of the Lagrange multipliers and, therefore, could facilitate the implementation of the algorithm and improve the condition number of the system. Indeed, since the boundary conditions on the contact boundary for the active nodes are directly enforced, we only get to solve a series of problems with simple boundary conditions, such as Dirichlet, Neumann or Robin boundary condition, based on the active set type method used. The purpose of the present work is to study and compare two active set type methods, the primal dual active set method and the projection iterative method, in the case of large and small deformation theories. The first one is the primal dual active set method used in various works such as [15, 16] and [18] and the reference therein. In [16], the Authors study a class of semismooth Newton methods for quadratic minimization problems to non negativity constraints in which global and local non-linear convergence results of the resulting primal dual active set strategy were established under strong assumptions on the matrix of the linearized systems. The proof is based on the M-matrix properties of the discrete operator; while such a statement is true for the Laplace operator it is not for the discrete elasticity operator, as the authors admitted. Furthermore, in that work, only linear elasticity problems with unilateral boundary constraints are considered. The work in [18] is devoted to provide an inexact primal dual active set approach to solve non-linear multibody contact problems for linear elasticity. The non-linearity of such problems arise only from the non penetration conditions for the involved bodies in contact. The second active set type method was used for instance in [29] to solve the so-called Signorini problem for the Laplace equations and to obtain a convergence analysis of the method. This active set method is based on a fixed point equation and can be formulated as a projection iterative algorithm. The projection iterative method consists to solve a sequence of Dirichlet or Robin boundary conditions according to a contact criteria in order to find the correct sets of active and inactive contact nodes. Our aim in this work is twofold. First, we present and analyse the active set type methods compared to the well-known augmented Lagrangian approach to solve a Signorini contact problem for hyperelasticity. Furthermore, we extend the convergence result obtained in [29] for the projection iterative method to a Signorini problem in the case of linear elasticity. Next we provide a numerical comparison of the different methods by considering simulations on two-dimensional test problems: one in the small deformation framework, the Hertz contact problem, and one in the large deformation framework, the contact between a hyperelastic ring and a rigid foundation under strong compressions. In particular, we analyze and compare the numerical convergence of the different methods with respect to several parameters such as the number of degrees of freedom or the number of iterations. By doing so, we also illustrate the behavior of the solution related to the contact condition.

The rest of the paper is structured as follows. In Section 2 we describe the contact conditions and introduce the mechanical problem in the large deformation framework. Then we introduce the notation and some preliminary material, list the assumptions on the data and state the variational

formulation of the problem in the hyperelasticity framework. In Section 3, we provide the finite element approximation of the variational formulation. After reformulating the problem into a minimization one, an augmented Lagrangian method is recalled to treat the unilateral constraints. In Section 4, we describe the two active set type methods used to solve unilateral contact problems in hyperelasticity: the primal dual active set method and the projection iterative method. The Section 5 is devoted to the convergence analysis of the projection iterative method to the solution of the Signorini Problem, in the small deformation hypothesis. After that, in Section 6 we present several numerical simulations to illustrate and compare the behavior of the two active set type methods. Finally, in Section 7, we conclude by recalling the results obtained and discussing about the conceivable works in the continuation of this one.

2. Formulations of the contact problem

The purpose of this section is to present both the mechanical problem and the variational formulation in the framework of hyperelasticity.

2.1. Hyperelastic contact model

The physical setting of the mechanical problem is as follows. A hyperelastic body occupies a bounded domain $\Omega \subset \mathbb{R}^d$ ($d = 1, 2, 3$) with a Lipschitz continuous boundary Γ , divided into three disjoint measurable parts Γ_1 , Γ_2 and Γ_3 such that $meas(\Gamma_1) > 0$. The notation $\mathbf{x} = (x_i)$ for a typical point in $\Omega \cup \Gamma$ is used and we denote by $\boldsymbol{\nu} = (\nu_i)$ the outward unit normal at Γ . Here and below the indices i, j, k, l run between 1 and d and, unless stated otherwise, the summation convention over repeated indices is used. We denote by \mathbb{M}^d the space of second order tensors on \mathbb{R}^d or, equivalently, the space of square matrices of order d . The inner product and norm on \mathbb{R}^d and \mathbb{M}^d are defined by

$$\begin{aligned} \mathbf{u} \cdot \mathbf{v} &= u_i v_i, & \|\mathbf{v}\| &= (\mathbf{v} \cdot \mathbf{v})^{\frac{1}{2}} & \forall \mathbf{u}, \mathbf{v} \in \mathbb{R}^d, \\ \mathbf{\Pi} \cdot \boldsymbol{\tau} &= \Pi_{ij} \tau_{ij}, & \|\boldsymbol{\tau}\| &= (\boldsymbol{\tau} \cdot \boldsymbol{\tau})^{\frac{1}{2}} & \forall \mathbf{\Pi}, \boldsymbol{\tau} \in \mathbb{M}^d. \end{aligned}$$

We use the notation \mathbf{u} and $\mathbf{\Pi}$ for the displacement field and the first Piola-Kirchhoff stress tensor, respectively. Also, we denote by u_ν and \mathbf{u}_τ the normal stress and tangential components of \mathbf{u} on Γ given by $u_\nu = \mathbf{v} \cdot \boldsymbol{\nu}$, $\mathbf{v}_\tau = \mathbf{v} - u_\nu \boldsymbol{\nu}$. Finally, Π_ν and $\mathbf{\Pi}_\tau$ will represent the normal and the tangential stress on Γ , defined by $\Pi_\nu = (\mathbf{\Pi} \boldsymbol{\nu}) \cdot \boldsymbol{\nu}$ and $\mathbf{\Pi}_\tau = \mathbf{\Pi} \boldsymbol{\nu} - \Pi_\nu \boldsymbol{\nu}$. Furthermore, an index that follows a comma represents the partial derivative with respect to the corresponding component of the spatial variable \mathbf{x} , e.g. $u_{i,j} = \partial u_i / \partial x_j$. Moreover, we recall that the divergence operator is defined by the equality $\text{Div } \mathbf{\Pi} = (\Pi_{ij,j})$.

In the problems studied below, the material's behavior is described with a hyperelastic constitutive law. We recall that hyperelastic constitutive laws are characterized by the first Piola-Kirchhoff tensor $\mathbf{\Pi}$ which derives from an internal hyperelastic energy density $W : \Omega \times \mathbb{M}_+^d \rightarrow \mathbb{R}$, $\mathbf{\Pi} = \frac{\partial}{\partial \mathbf{F}} W(\mathbf{x}, \mathbf{F}) = \partial_{\mathbf{F}} W(\mathbf{x}, \mathbf{F})$, for all $\mathbf{x} \in \Omega$ and $\mathbf{F} \in \mathbb{M}^d$. Here \mathbf{F} is the deformation gradient defined by $\mathbf{F} = \mathbf{I} + \nabla \mathbf{u}$ and $\partial_{\mathbf{F}}$ represents the differential with respect to the variable \mathbf{F} , see [8, 22] for details on hyperelasticity. In what follows, we consider the contact without friction of a hyperelastic body with a perfectly rigid obstacle, the so-called foundation. The hyperelastic body is in equilibrium under the action of body forces of density \mathbf{f}_0 and surface tractions of density \mathbf{f}_2 which act on Γ_2 . We also assume that the body is fixed on Γ_1 and may come in contact over Γ_3 with the foundation. The frictionless contact conditions are based on the unilateral contact conditions without friction

and can be written following the Karush-Kuhn-Tucker conditions on Γ_3 :

$$u_\nu \leq 0, \quad (2.1)$$

$$\Pi_\nu \leq 0, \quad (2.2)$$

$$u_\nu \Pi_\nu = 0, \quad (2.3)$$

$$\mathbf{\Pi}_\tau = 0. \quad (2.4)$$

With these preliminaries, the formulation of the contact problem we consider in this work is as follows.

Problem \mathcal{P} . Find a displacement field $\mathbf{u} : \Omega \rightarrow \mathbb{R}^d$ and a stress field $\mathbf{\Pi} : \Omega \rightarrow \mathbb{M}^d$ such that

$$\mathbf{\Pi} = \partial_{\mathbf{F}} W(\mathbf{F}) \quad \text{in } \Omega, \quad (2.5)$$

$$\text{Div } \mathbf{\Pi} + \mathbf{f}_0 = \mathbf{0} \quad \text{in } \Omega, \quad (2.6)$$

$$\mathbf{u} = \mathbf{0} \quad \text{on } \Gamma_1, \quad (2.7)$$

$$\mathbf{\Pi} \boldsymbol{\nu} = \mathbf{f}_2 \quad \text{on } \Gamma_2, \quad (2.8)$$

$$u_\nu \leq 0, \quad \Pi_\nu \leq 0, \quad u_\nu \Pi_\nu = 0 \quad \text{on } \Gamma_3, \quad (2.9)$$

$$\mathbf{\Pi}_\tau = \mathbf{0} \quad \text{on } \Gamma_3. \quad (2.10)$$

Here and below, in order to simplify the notation, we do not indicate explicitly the dependence of various functions on the spatial variable \mathbf{x} . Equation (2.5) represents the hyperelastic constitutive law of the material. Equation (2.6) is the equation of equilibrium in the static case. Conditions (2.7) and (2.8) represent the displacement and traction boundary conditions, respectively. Finally, conditions (2.9) and (2.10) represent the frictionless contact conditions with unilateral constraint previously described in this section. Note that the conditions (2.9) are equivalent to the following subdifferential inclusion (cf [23])

$$-\Pi_\nu \in \partial \Psi_{\mathbb{R}^-}(u_\nu) \quad \text{on } \Gamma_3, \quad (2.11)$$

where ∂ represents the subdifferential operator in the sense of the convex analysis and Ψ_A denotes the indicator function of the set $A \subset \mathbb{R}$.

2.2. Variational formulation

In order to derive the variational formulation of Problem \mathcal{P} , also called in the literature the Signorini Problem, further notation and some preliminary material are needed. Everywhere in this paper, the standard notations for Sobolev and Lebesgue spaces associated to Ω and Γ are used. The following spaces are considered

$$V = \{\mathbf{v} \in H^1(\Omega; \mathbb{R}^d) : \mathbf{v} = \mathbf{0} \text{ on } \Gamma_1\}, \quad H = L^2(\Omega; \mathbb{R}^d).$$

These are real Hilbert spaces endowed with their standard inner products $\langle \mathbf{u}, \mathbf{v} \rangle_V$ and $\langle \mathbf{\Pi}, \boldsymbol{\tau} \rangle_H$ and their associated norms $\|\cdot\|_V$ and $\|\cdot\|_H$, respectively. Note that $V \subset H \subset V^*$ is an evolution triple, with all embeddings being continuous, compact and dense. The duality pairing between V^* and V will be denoted by $\langle \mathbf{u}, \mathbf{v} \rangle_{V^* \times V}$. Also, recall that $H_1 = H^1(\Omega)^d$ algebraically and topologically. Completeness of the space $(V, \|\cdot\|_V)$ follows from the assumption $meas(\Gamma_1) > 0$, which allows the

use of Korn's inequality. We also recall that there exists $c_0 > 0$ which depends on Ω , Γ_1 and Γ_3 such that

$$\|\mathbf{v}\|_{L^2(\Gamma_3)^d} \leq c_0 \|\mathbf{v}\|_V \quad \text{for all } \mathbf{v} \in V. \quad (2.12)$$

Inequality (2.12) represents a consequence of the Sobolev trace theorem. It is well known that the weak solution of problem \mathcal{P} can be defined from a variational inequality [17, 20], or can be obtained equivalently from a minimization problem on a convex set, see [6, 13]. In this section, a saddle point formulation within the form of a hybrid variational formulation is considered. In this case, the Lagrange multiplier λ_ν related to the contact stress verifies an extended subdifferential inclusion derived from the pointwise subdifferential inclusion defined in (2.11). Note that, for convenience, the Lagrange multiplier λ_ν is taken as equal to $-\Pi_\nu$. To this end, a trace space is defined by $X_\nu = \{v_\nu|_{\Gamma_3} : \mathbf{v} \in V\}$ equipped with its usual norms. We denote by X'_ν the duals of the spaces X_ν . Moreover, we denote by $\langle \cdot, \cdot \rangle_{X'_\nu, X_\nu}$ the corresponding duality pairing mapping. Then a function $\varphi_\nu : X_\nu \rightarrow (-\infty, +\infty]$ is introduced, defined by

$$\varphi_\nu(v_\nu) = \int_{\Gamma_3} \Psi_{\mathbb{R}^-}(v_\nu) d\Gamma \quad \forall v_\nu \in X_\nu.$$

Therefore, the pointwise inclusion condition (2.11) leads to the extended subdifferential inclusion

$$\lambda_\nu \in \partial\varphi_\nu(u_\nu) \quad \text{in } X'_\nu. \quad (2.13)$$

For an element $\mathbf{v} \in H_1$, \mathbf{v} is still written for the trace of \mathbf{v} . Also, for a regular stress function $\mathbf{\Pi}$ the following Green's formula holds:

$$\int_{\Omega} \mathbf{\Pi} : \nabla \mathbf{v} dx + \int_{\Omega} \text{Div } \mathbf{\Pi} \cdot \mathbf{v} dx = \int_{\Gamma} \mathbf{\Pi} \boldsymbol{\nu} \cdot \mathbf{v} da \quad \text{for all } \mathbf{v} \in H_1. \quad (2.14)$$

Moreover, in the study of the mechanical problem (2.5)–(2.10) we assume that the body forces and tractions densities have the regularity

$$\mathbf{f}_0 \in L^2(\Omega)^d, \quad \mathbf{f}_2 \in L^2(\Gamma_2)^d. \quad (2.15)$$

Now we turn to the hybrid variational formulation of Problem \mathcal{P} . To this end, we introduce the non linear hyperelastic operator $A : V \rightarrow V^*$, and the element \mathbf{f} defined by

$$\langle A(\mathbf{u}), \mathbf{v} \rangle_{V^* \times V} = \int_{\Omega} \mathbf{\Pi} : \nabla \mathbf{v} dx \quad \forall \mathbf{u}, \mathbf{v} \in V, \quad (2.16)$$

$$(\mathbf{f}, \mathbf{v})_V = (\mathbf{f}_0, \mathbf{v})_H + (\mathbf{f}_2, \mathbf{v})_{L^2(\Gamma_2)}, \quad \forall \mathbf{v} \in V. \quad (2.17)$$

We use Green's formula (2.14) and definition (2.17) to see that

$$\langle A(\mathbf{u}), \mathbf{v} \rangle_{V^* \times V} = (\mathbf{f}, \mathbf{v})_V + \int_{\Gamma_3} \Pi_\nu v_\nu da + \int_{\Gamma_3} \mathbf{\Pi}_\tau \cdot \mathbf{v}_\tau da.$$

Then by using the Lagrange multiplier λ_ν , related to the normal contact stress Π_ν , and the condition (2.10), we obtain the variational formulation of the frictionless contact problem \mathcal{P} in terms of two unknown fields.

Problem \mathcal{P}_V . Find a displacement field \mathbf{u} and a normal stress field $\boldsymbol{\lambda} = \lambda_\nu \boldsymbol{\nu}$ such that

$$\mathbf{u} \in V, \quad \langle A(\mathbf{u}), \mathbf{v} \rangle_{V^* \times V} + \langle \lambda_\nu, v_\nu \rangle_{X'_\nu, X_\nu} = (\mathbf{f}, \mathbf{v})_V \quad \forall \mathbf{v} \in V, \quad (2.18)$$

$$\lambda_\nu \in \partial\varphi_\nu(u_\nu) \quad \text{in } X'_\nu. \quad (2.19)$$

A pair $(\mathbf{u}, \boldsymbol{\lambda})$ which satisfies (2.18), (2.19) and the hyperelastic constitutive law in the form $\mathbf{\Pi} = \partial_{\mathbf{F}} W(\mathbf{F})$ is called a *weak solution* to the frictionless contact problem \mathcal{P} .

The solvability of the Problem \mathcal{P}_V can be obtained by using an existence result for a three dimensional hyperelastic Signorini contact problem, provided in [8, p.381]. The result recalled below is based on the polyconvexity and the coerciveness of the stored density energy W .

Theorem 2.1. (existence result for a Signorini contact problem) Let Ω be a domain in \mathbb{R}^3 , and let $W : \Omega \times \mathbb{M}_+^3 \rightarrow \mathbb{R}^+$ be a stored energy function with the following properties:
(a) *Polyconvexity:* For almost all $x \in \Omega$, there exists a convex function $\mathbb{W}(\mathbf{x}, \cdot) : \mathbb{M}^3 \times \mathbb{M}^3 \times \mathbb{R}^{+*} \rightarrow \mathbb{R}$ such that

$$\mathbb{W}(\mathbf{x}, \mathbf{F}, \text{Cof } \mathbf{F}, \det \mathbf{F}) = W(\mathbf{x}, \mathbf{F}) \quad \text{for all } \mathbf{F} \in \mathbb{M}_+^3; \quad (2.20)$$

the function $\mathbb{W}(\cdot, \mathbf{F}, \mathbf{H}, \delta) : \Omega \rightarrow \mathbb{R}$ is measurable for all $(\mathbf{F}, \mathbf{H}, \delta) \in \mathbb{M}^3 \times \mathbb{M}^3 \times \mathbb{R}^{+*}$.

(b) $\lim_{\det \mathbf{F} \rightarrow 0^+} W(\mathbf{x}, \mathbf{F}) = +\infty$, for almost all $\mathbf{x} \in \Omega$.

(c) *Coerciveness:* There exist constants α, β, p, q, r such that

$$\alpha > 0, \quad p \geq 2, \quad q \geq \frac{p}{p-1}, \quad r > 1, \quad (2.21)$$

$$W(\mathbf{x}, \mathbf{F}) \geq \alpha(\|\mathbf{F}\|^p + \|\text{Cof } \mathbf{F}\|^q + \|\det \mathbf{F}\|^r) + \beta \quad (2.22)$$

for almost all $x \in \Omega$ and for all $\mathbf{F} \in \mathbb{M}^3$.

Let Γ_1, Γ_2 and Γ_3 be disjoint relatively open subset of Γ with $\text{meas}(\Gamma_1) > 0$ and $\text{meas}(\{\Gamma - (\Gamma_1 \cup \Gamma_2 \cup \Gamma_3)\}) = 0$, and let $\mathbf{u}_0 : \Gamma_1 \rightarrow \mathbb{R}^3$ be a measurable function such that the set

$$\begin{aligned} \Phi = \{ \mathbf{v} \in W^{1,p}(\Omega); \text{Cof } \nabla \mathbf{v} \in L^q(\Omega), \det \nabla \mathbf{v} \in L^r(\Omega), \\ \mathbf{v} = \mathbf{u}_0 \text{ on } \Gamma_1, \det \nabla \mathbf{v} > 0 \text{ a.e. in } \Omega \} \end{aligned}$$

is nonempty. Let the linear form L defined by $L(\mathbf{v}) = (\mathbf{f}, \mathbf{v})_V$ be continuous on $W^{1,p}(\Omega)$. Finally, let $I(\mathbf{v}) = \int_{\Gamma_3} \Psi_{\mathbb{R}^-}(v_\nu) d\Gamma - L(\mathbf{v})$, and assume that $\inf_{\mathbf{v} \in \Phi} I(\mathbf{v}) < +\infty$. Then there exists at least one function \mathbf{u} such that

$$\mathbf{v} \in \Phi \text{ and } I(\mathbf{v}) = \inf_{\mathbf{v} \in \Phi} I(\mathbf{v}). \quad (2.23)$$

Remark 1. The solvability of problem \mathcal{P}_V can be obtained directly by applying the Theorem 2.1 in the case where $p = 2, q = 2, r = 2$ and $\mathbf{u}_0 = \mathbf{0}$. It is easy to see that problem \mathcal{P}_V with $d = 3$ can be derived from the minimization problem (2.23), see [2, 8, 22].

Remark 2. In the case of linear elasticity, if we assume that the elasticity operator is a strongly monotone Lipschitz continuous operator on the space V (which is not true for hyperelasticity) then, as proved in [27, p. 126], for each $f \in V$ there is a unique weak solution to the contact problem \mathcal{P}_V .

3. Variational approximation and Lagrangian method

This section is devoted to provide a discrete minimization approach in order to solve the variational problem \mathcal{P}_V . To this end, first the discretization of the variational Problem \mathcal{P}_V is presented and next, the augmented Lagrangian approach based on an optimization formulation is recalled.

3.1. Discretization step

Let Ω be a polyhedral domain. Moreover, let $\{\mathcal{T}^h\}$ be a regular family of triangular finite element partitions of $\bar{\Omega}$ that are compatible with the boundary decomposition $\Gamma = \bar{\Gamma}_1 \cup \bar{\Gamma}_2 \cup \bar{\Gamma}_3$, i.e., if one side of an element $Tr \in \mathcal{T}^h$ has more than one point on Γ , then the side lies entirely on $\bar{\Gamma}_1, \bar{\Gamma}_2$ or $\bar{\Gamma}_3$. The space V is approximated by the finite dimensional space $V^h \subset V$ of continuous and piecewise affine functions, that is,

$$\begin{aligned} V^h = \{ \mathbf{v}^h \in [C(\bar{\Omega})]^d : \mathbf{v}^h|_{Tr} \in [P_1(Tr)]^d \quad \forall Tr \in \mathcal{T}^h, \\ \mathbf{v}^h = \mathbf{0} \text{ at the nodes on } \Gamma_1 \}, \end{aligned}$$

where $P_1(Tr)$ represents the space of polynomials of degree less or equal to one in Tr and $h > 0$ denotes the spatial discretization parameter. For the discretization of the Lagrange multiplier space X'_ν , we use discontinuous piecewise constant functions as it is done in [3, 19]. The discrete Lagrange multiplier space is denoted by Y_ν^h . Thus, let us consider the following discrete variational problem. **Problem \mathcal{P}_V^h .** Find a discrete displacement field \mathbf{u}^h and a discrete normal stress field $\boldsymbol{\lambda}^h = \lambda_\nu^h \boldsymbol{\nu}$ such that

$$\mathbf{u}^h \in V^h, \quad \langle A(\mathbf{u}^h), \mathbf{v}^h \rangle_{V^* \times V} + \langle \lambda_\nu^h, v_\nu^h \rangle_{X'_\nu \times X_\nu} = (\mathbf{f}, \mathbf{v}^h)_V \quad \forall \mathbf{v}^h \in V^h, \quad (3.1)$$

$$\lambda_\nu^h \in \partial \varphi_\nu(u_\nu^h) \quad \text{in } Y_\nu^h. \quad (3.2)$$

For details about the discrete formulation, we refer, e.g., to [4, 5, 21, 28].

3.2. Minimization formulation and augmented Lagrangian method

The discrete weak solutions of Problem \mathcal{P}_V^h can also be obtained from a minimization problem on a convex set which leads to an unconstrained augmented Lagrangian method. This method was described in detail in [1, 21, 28]. The starting point of this formulation is to consider the following optimization problem.

$$\mathbf{u}^h = \operatorname{argmin}_{\mathbf{v}^h \in V^h} \left\{ J(\mathbf{v}^h) + \varphi_\nu(v_\nu^h) \right\}, \quad (3.3)$$

where $J(\mathbf{v}^h)$ is the hyperelastic strain energy potential defined by

$$J(\mathbf{v}^h) = \frac{1}{2} \langle A(\mathbf{v}^h), \mathbf{v}^h \rangle_{V^* \times V} - (\mathbf{f}, \mathbf{v}^h)_V. \quad (3.4)$$

Therefore, with the formalism of the standard Lagrangian, the problem (3.4) is equivalent to the minmax problem

$$(\mathbf{u}^h, \lambda_\nu^h) \in \operatorname{arg}(\min_{\mathbf{v}^h} \max_{\gamma_\nu^h \in \mathbb{R}^+} \{L(\mathbf{v}^h, \gamma_\nu^h)\}), \quad (3.5)$$

where $\lambda_\nu^h \in Y^h \cap \mathbb{R}^+$ stands for the Lagrange multiplier while γ_ν^h is the virtual Lagrange variable, which represents the normal contact stress. The Lagrangian function L is defined by

$$L(\mathbf{v}^h, \gamma_\nu^h) = J(\mathbf{v}^h) + \langle v_\nu^h, \gamma_\nu^h \rangle_{X_\nu \times X'_\nu}. \quad (3.6)$$

We use now an augmented Lagrangian approach which permits to derive a smooth minimization problem without constraints. At this point, the regularized augmented Lagrangian expression is given by

$$L_r(\mathbf{v}^h, \gamma_\nu^h) = J(\mathbf{v}^h) - \frac{1}{2r} \|\gamma_\nu^h\|^2 + \frac{1}{2r} [\gamma_\nu^h + r v_\nu^h]_+^2, \quad (3.7)$$

with $r > 0$, a penalty factor and $[\cdot]_+$, the positive part of an element of \mathbb{R} i.e. $[a]_+ = \max(a, 0)$ for $a \in \mathbb{R}$. Then the following augmented Lagrangian minimization problem is obtained

$$(\mathbf{u}^h, \lambda_\nu^h) \in \operatorname{arg}(\min \{L_r(\mathbf{v}^h, \gamma_\nu^h)\}), \text{ where } \mathbf{v}^h \in V^h \text{ and } \gamma_\nu^h \in Y_\nu^h. \quad (3.8)$$

Assuming that J is continuously differentiable with respect to \mathbf{v} and strictly convex, L_r is continuously differentiable with respect to \mathbf{v}^h and γ_ν^h and therefore, a saddle-point $(\mathbf{u}^h, \lambda_\nu^h)$ verifies the following stationary condition

$$\nabla_{\mathbf{u}^h, \lambda_\nu^h} L_r(\mathbf{u}^h, \lambda_\nu^h) = \mathbf{0}. \quad (3.9)$$

It leads to a system of non linear equations of the form

$$\begin{cases} \nabla_{\mathbf{u}^h} L_r(\mathbf{u}^h, \lambda_\nu^h) = \nabla_{\mathbf{u}^h} J(\mathbf{u}^h) + [\lambda_\nu^h + r u_\nu^h]_+ \boldsymbol{\nu} = \mathbf{0}, \\ \nabla_{\lambda_\nu^h} L_r(\mathbf{u}^h, \lambda_\nu^h) = -\frac{1}{r} \left\{ \lambda_\nu^h - [\lambda_\nu^h + r u_\nu^h]_+ \right\} = 0. \end{cases}$$

Note that from now on, in order to simplify the notation, we do not indicate explicitly the spatial discretization parameter on the unknown fields. We denote by \mathbf{u} and $\boldsymbol{\lambda}$ the vectors representing the generalized vectors of displacement and Lagrange multiplier, defined by $\mathbf{u} = \{\mathbf{u}^i\}_{i=1}^{N_{Tot}^h}$ and $\boldsymbol{\lambda} = \{\boldsymbol{\lambda}^i\}_{i=1}^{N_{\Gamma_3}^h}$, respectively, with N_{Tot}^h , the number of nodes of the discretization of Ω and $N_{\Gamma_3}^h$, the number of nodes of the discretization of Γ_3 . Here, \mathbf{u}^i represents the value of the corresponding function \mathbf{u}^h at the i^{th} nodes of \mathcal{T}^h while $\boldsymbol{\lambda}^i$ denotes the value of the corresponding function $\boldsymbol{\lambda}^h = \lambda_\nu^h \boldsymbol{\nu}$ at the i^{th} nodes arising from the discretization of the contact interface Γ_3 denoted by Γ_3^h . Therefore, by adopting a vector form, we have the following system of non linear equations:

Problem \mathcal{P}_L . Find a displacement field $\mathbf{u} \in \mathbb{R}^{d \times N_{Tot}^h}$ and a normal stress field $\boldsymbol{\lambda} = \lambda_\nu \boldsymbol{\nu} \in \mathbb{R}^{d \times N_{\Gamma_3}^h}$ such that

$$G(\mathbf{u}) + \mathcal{F}(\mathbf{u}, \lambda_\nu) = \mathbf{0}_{d \times N_{Tot}^h + N_{\Gamma_3}^h}, \quad (3.10)$$

where $G(\mathbf{u}) \in \mathbb{R}^{d \times N_{Tot}^h} \times \mathbb{R}^{N_{\Gamma_3}^h}$ is the hyperelastic part and $\mathcal{F}(\mathbf{u}, \boldsymbol{\lambda}) \in \mathbb{R}^{d \times N_{Tot}^h} \times \mathbb{R}^{N_{\Gamma_3}^h}$ is the non differentiable contact part defined as follows

$$G(\mathbf{u}) = \begin{pmatrix} A(\mathbf{u}) - \mathbf{f} \\ \mathbf{0}_{N_{\Gamma_3}^h} \end{pmatrix} \quad \text{and} \quad \mathcal{F}(\mathbf{u}, \lambda_\nu) = \begin{pmatrix} [\lambda_\nu + r u_\nu]_+ \boldsymbol{\nu} \\ -\frac{1}{r} \{ \lambda_\nu - [\lambda_\nu + r u_\nu]_+ \} \end{pmatrix},$$

here $\mathbf{0}_{N_{\Gamma_3}^h}$ is the zero of $\mathbb{R}^{N_{\Gamma_3}^h}$ and $\mathbf{0}_{d \times N_{Tot}^h + N_{\Gamma_3}^h}$ is the zero of $\mathbb{R}^{d \times N_{Tot}^h + N_{\Gamma_3}^h}$.

The solution of the non linear Problem \mathcal{P}_L is based on a generalized Newton method which permits to treat both variables $(\mathbf{u}, \boldsymbol{\lambda})$ simultaneously. Now, by considering the pair $\mathbf{x} = (\mathbf{u}, \boldsymbol{\lambda})$, the iterative scheme of index k can be summarized as follows.

(i) Choose \mathbf{x}^0 , set $k = 0$.

(ii) Set $\mathbf{x}^{(k+1)}$, such that

$$\mathbf{x}^{(k+1)} = \mathbf{x}^{(k)} - (K_k + L_k)^{-1} (G(\mathbf{x}^{(k)}) + \mathcal{F}(\mathbf{x}^{(k)})), \quad L_k \in \partial \mathcal{F}(\mathbf{x}^{(k)}), \quad (3.11)$$

where $\partial \mathcal{F}(\mathbf{x}^{(k)})$ is the generalized Jacobian of \mathcal{F} at $\mathbf{x}^{(k)}$ and K_k is the Jacobian of G at $\mathbf{x}^{(k)}$.

(iii) If $\|\mathbf{x}^{(k+1)} - \mathbf{x}^{(k)}\| \leq \epsilon$ and $\|\mathcal{R}^L(\mathbf{x}^{(k)})\| \leq \epsilon$ then stop, else goto (ii).

Here, ϵ represents a small value and $\mathcal{R}^L(\mathbf{x}^{(k)})$ is the nonlinear operator belonging to $\mathbb{R}^{d \times N_{Tot}^h} \times \mathbb{R}^{N_{\Gamma_3}^h}$, defined by

$$\mathcal{R}^L(\mathbf{x}^{(k)}) = G(\mathbf{u}^{(k)}) + \mathcal{F}(\mathbf{u}^{(k)}, \boldsymbol{\lambda}^{(k)}).$$

Remark 3. This method requires the consideration of additional immaterial nodes associated to the Lagrange multipliers, for the treatment of the contact operator $\mathcal{F}(\mathbf{u}, \boldsymbol{\lambda})$. The construction of these fictitious nodes depends on the contact element used for the geometrical discretization of the interface Γ_3 . In the case of the numerical examples presented in Section 6, the discretization is based on “node-to-rigid” contact element, which is composed by one node of Γ_3^h and one Lagrange multiplier node.

4. Active set type methods

The aim of this section is to present the main traits of two active set type methods used to solve unilateral contact problems without friction between a hyperelastic body and a rigid obstacle. These two methods are the primal dual active set method and the projection iterative method. See [18] and [29] for a presentation of the methods in the case of linear elasticity and Laplace equations, respectively. Then, in each case, we present the method and detail the associated iterative algorithm for the hyperelastic Signorini problem.

4.1. Primal dual active set

The primal dual active set type method can be seen as a semismooth Newton method based on the reformulation of conditions (2.9), see [16]. As a matter of fact, the unilateral contact conditions (2.9) can be formulated in terms of a fixed point problem, as mentioned in [7]. Let us recall and prove this result.

Proposition 4.1. *Let $\gamma > 0$, the unilateral contact conditions (2.9) are equivalent to:*

$$\Pi_\nu = -[-\Pi_\nu + \gamma u_\nu]_+ \quad \text{on } \Gamma_3. \quad (4.1)$$

Proof. Let's assume that (2.9) hold. Then, either $u_\nu < 0$ or $u_\nu = 0$. First, if $u_\nu < 0$, (2.3) implies that $\Pi_\nu = 0$. So

$$-[-\Pi_\nu + \gamma u_\nu]_+ = -[\gamma u_\nu]_+ = 0 \quad \text{and} \quad \Pi_\nu = 0 \implies \Pi_\nu = -[-\Pi_\nu + \gamma u_\nu]_+.$$

Suppose now that $u_\nu = 0$ and $\Pi_\nu < 0$

$$-[-\Pi_\nu + \gamma u_\nu]_+ = -[-\Pi_\nu]_+ = \Pi_\nu.$$

Conversely, if (4.1) holds, it implies that (2.2) holds. Next, if $\Pi_\nu = 0$ we have

$$-[\gamma u_\nu]_+ = 0,$$

which means that $u_\nu < 0$, since $\gamma > 0$. At last, if $\Pi_\nu < 0$, $-\Pi_\nu + \gamma u_\nu > 0$ and

$$\Pi_\nu = -[-\Pi_\nu + \gamma u_\nu]_+ = \Pi_\nu - \gamma u_\nu,$$

so $\gamma u_\nu = 0$ and, since $\gamma > 0$, $u_\nu = 0$. Therefore (2.1) and (2.3) hold, which concludes the proof. \square

Now, let $(\mathbf{u}, \boldsymbol{\lambda})$ be the solution of the discrete variational problem \mathcal{P}_V^h , with λ_ν the Lagrange multiplier introduced in the previous part and defined by $\lambda_\nu = -\Pi_\nu$. The Problem \mathcal{P}_V^h can be rewritten in a discrete algebraic form with the condition (4.1) for the Lagrange multiplier. Then, it leads to consider the system of non linear equations of the following form

$$\mathcal{R}(\mathbf{u}, \boldsymbol{\lambda}) = \begin{pmatrix} \mathcal{R}^{\mathbf{u}}(\mathbf{u}, \boldsymbol{\lambda}) = A(\mathbf{u}) + \lambda_\nu \nu - \mathbf{f} \\ \mathcal{R}^{\boldsymbol{\lambda}}(\mathbf{u}, \boldsymbol{\lambda}) = \lambda_\nu - [\lambda_\nu + \gamma u_\nu]_+ \end{pmatrix} = \begin{pmatrix} \mathbf{0} \\ 0 \end{pmatrix}, \quad (4.2)$$

where, $\mathcal{R}(\mathbf{u}, \boldsymbol{\lambda})$ is the generalized non linear operator belonging to $\mathbb{R}^{d \times N_{Tot}^h} \times \mathbb{R}^{N_{\Gamma_3}^h}$. Therefore, by adopting the semismooth Newton formalism, the solution $(\mathbf{u}, \boldsymbol{\lambda})$ can be formulated as follows:

(i) Choose $(\mathbf{u}^{(0)}, \boldsymbol{\lambda}^{(0)})$, set $k = 0$.

(ii) Set $(\mathbf{u}^{(k+1)}, \boldsymbol{\lambda}^{(k+1)})$ such that

$$\mathcal{G}^{\mathbf{u}}(\mathbf{u}^{(k)}, \boldsymbol{\lambda}^{(k)}) \delta \mathbf{u}^{(k)} = -\mathcal{R}^{\mathbf{u}}(\mathbf{u}^{(k)}, \boldsymbol{\lambda}^{(k)}), \quad (4.3)$$

$$\Delta \mathcal{R}^{\boldsymbol{\lambda}}(\mathbf{u}^{(k)}, \boldsymbol{\lambda}^{(k)}) = -\mathcal{R}^{\boldsymbol{\lambda}}(\mathbf{u}^{(k)}, \boldsymbol{\lambda}^{(k)}), \quad (4.4)$$

$$\mathbf{u}^{(k+1)} = \mathbf{u}^{(k)} + \delta \mathbf{u}^{(k)}, \quad (4.5)$$

$$\boldsymbol{\lambda}^{(k+1)} = \boldsymbol{\lambda}^{(k)} + \delta \boldsymbol{\lambda}^{(k)}, \quad (4.6)$$

where $\mathcal{G}^{\mathbf{u}}(\mathbf{u}^{(k)}, \boldsymbol{\lambda}^{(k)})$ stands for the differential of $\mathcal{R}^{\mathbf{u}}$ with respect to the variable $\mathbf{u}^{(k)}$ as follows

$$\mathcal{G}^{\mathbf{u}}(\mathbf{u}^{(k)}, \boldsymbol{\lambda}^{(k)}) = \frac{\partial \mathcal{R}^{\mathbf{u}}(\mathbf{u}^{(k)}, \boldsymbol{\lambda}^{(k)})}{\partial \mathbf{u}^{(k)}},$$

and $\Delta \mathcal{R}^{\boldsymbol{\lambda}}(\mathbf{u}^{(k)}, \boldsymbol{\lambda}^{(k)})$ represents the total differential of the complementarity function $\mathcal{R}^{\boldsymbol{\lambda}}$ with respect to the variables $\mathbf{u}^{(k)}$ and $\boldsymbol{\lambda}^{(k)}$ as follows

$$\Delta \mathcal{R}^{\boldsymbol{\lambda}}(\mathbf{u}^{(k)}, \boldsymbol{\lambda}^{(k)}) = \frac{\partial \mathcal{R}^{\boldsymbol{\lambda}}(\mathbf{u}^{(k)}, \boldsymbol{\lambda}^{(k)})}{\partial (\mathbf{u}^{(k)}, \boldsymbol{\lambda}^{(k)})} (\delta \mathbf{u}^{(k)}, \delta \boldsymbol{\lambda}^{(k)}).$$

(iii) If $\|(\mathbf{u}^{(k+1)}, \boldsymbol{\lambda}^{(k+1)}) - (\mathbf{u}^{(k)}, \boldsymbol{\lambda}^{(k)})\| \leq \epsilon$ and $\|\mathcal{R}(\mathbf{u}^{(k)}, \boldsymbol{\lambda}^{(k)})\| \leq \epsilon$ then stop, else goto (ii).

The main traits of this method is to consider separately the solution of $\mathcal{R}(\mathbf{u}, \boldsymbol{\lambda}) = \mathbf{0}$ and the fixed point $\lambda_\nu = [\lambda_\nu + \gamma u_\nu]_+$ which is determined by equation (4.4). Let us denote by \mathcal{S} the set of all nodes of the finite element mesh belonging to Γ_3^h and p a node of \mathcal{S} . After some calculus of variations, it is easy to see that the equation (4.4) leads directly to enforce $u_{\nu,p} = 0$ if the nodes $p \in \mathcal{S}$ are in status of contact by checking an active set condition that is $\lambda_{\nu,p} + \gamma u_{\nu,p} \geq 0$ for all $p \in \mathcal{S}$. Furthermore, equation (4.4) leads also to the condition $\lambda_{\nu,p} = 0$ in the case of non contact, see [15, 16] for more details. Thereby, let us consider the active subset \mathcal{A} of contact nodes defined by $\mathcal{A} = \{p \in \mathcal{S} : \lambda_{\nu,p} + \gamma u_{\nu,p} \geq 0\}$, and the associated inactive subset: $\mathcal{I} = \mathcal{S} \setminus \mathcal{A}$. Now, we turn to the description of the iterative active set algorithm of index k .

(i) Choose $(\mathbf{u}^{(0)}, \boldsymbol{\lambda}^{(0)})$, set $k = 0$.

(ii) Set $\mathcal{A}_{k+1} = \{p \in \mathcal{S} : \lambda_{\nu,p}^{(k)} + \gamma u_{\nu,p}^{(k)} \geq 0\}$, $\mathcal{I}_{k+1} = \mathcal{S} \setminus \mathcal{A}_{k+1}$.

(iii) Find $(\mathbf{u}^{(k+1)}, \boldsymbol{\lambda}^{(k+1)})$ such that

$$\begin{aligned} \mathbf{u}^{(k+1)} &= \mathbf{u}^{(k)} - [\mathcal{G}(\mathbf{u}^{(k)}, \boldsymbol{\lambda}^{(k)})]^{-1} \mathcal{R}(\mathbf{u}^{(k)}, \boldsymbol{\lambda}^{(k)}) \\ u_{\nu,p}^{(k+1)} &= 0 \quad \text{for all } p \in \mathcal{A}_{k+1}, \end{aligned} \quad (4.7)$$

$$\lambda_{\nu,p}^{(k+1)} = 0 \quad \text{for all } p \in \mathcal{I}_{k+1}. \quad (4.8)$$

(iv) If $\|(\mathbf{u}^{(k+1)}, \boldsymbol{\lambda}^{(k+1)}) - (\mathbf{u}^{(k)}, \boldsymbol{\lambda}^{(k)})\| \leq \epsilon$, $\|\mathcal{R}(\mathbf{u}^{(k+1)}, \boldsymbol{\lambda}^{(k+1)})\| \leq \epsilon$ and $\mathcal{A}_{k+1} = \mathcal{A}_k$ then stop, else goto (ii).

We recall that the aim of the active set type strategy is to find the correct subset \mathcal{A} of all nodes that are currently in contact with the perfectly rigid obstacle.

Remark 4. *Unlike the augmented Lagrangian approach, another traits of the active set type method is the non-use of additional nodes for the determination of the normal contact stress. The computation of $\lambda_{\nu,p}^{(k+1)}$ for all $p \in \mathcal{A}_{k+1}$ is obtained a posteriori by using the solution $\mathbf{u}^{(k+1)}$ in the equation $A(\mathbf{u}^{(k+1)}) + \lambda_\nu^{(k+1)} \nu = \mathbf{f}$. Nevertheless, we can note a similarity with the augmented Lagrangian method. Indeed, the second equation of (4.2) corresponds exactly to the second equation of (3.10).*

4.2. Projection iterative method

In this part, a projection iterative algorithm based on a fixed point equation is presented. Note that in (4.1) we used a reformulation of the unilateral contact conditions in the term of a nonlinear complementary problem function. Here, in order to obtain the adequate fixed point equation, this function can be used slightly differently to obtain another formulation of (2.9). Indeed, let $c > 0$, the Signorini boundary conditions (2.9) are equivalent to the following fixed point problem:

$$u_\nu = -[-u_\nu + c\Pi_\nu]_+ \text{ on } \Gamma_3. \quad (4.9)$$

Remark that the equivalence between (4.9) and (4.1) can be easily proved by similar arguments that those used in Section 4.1. Then, the discrete variational problem \mathcal{P}_V^h can be rewritten in another equivalent discrete algebraic form, as follows

$$A(\mathbf{u}) + \lambda_\nu \nu = \mathbf{f}, \quad (4.10)$$

$$u_{\nu,p} + [-u_{\nu,p} - c\lambda_{\nu,p}]_+ = 0 \quad \text{for all } p \in \mathcal{S}. \quad (4.11)$$

Using (4.11), an implicit scheme of index k on \mathcal{S} is used and it can be formulated as follows

$$u_{\nu,p}^{(k+1)} = -[-u_{\nu,p}^{(k)} - c\lambda_{\nu,p}^{(k+1)}]_+, \quad \text{for all } p \in \mathcal{S}. \quad (4.12)$$

Note that an explicit scheme for the numerical treatment of (4.11) could also be used, but with all the drawbacks inherent in this type of method.

Now, we turn to the description of the projection iterative algorithm (see [29] for a presentation in the case of Laplace equations with a unilateral constraint).

- (i) Choose $(\mathbf{u}^{(0)}, \boldsymbol{\lambda}^{(0)})$, set $k = 0$.
- (ii) Set $\mathcal{A}_{k+1} = \{p \in \mathcal{S} : u_{\nu,p}^{(k)} + c\lambda_{\nu,p}^{(k)} \geq 0\}$, $\mathcal{I}_{k+1} = \mathcal{S} \setminus \mathcal{A}_{k+1}$.
- (iii) Find $(\mathbf{u}^{(k+1)}, \boldsymbol{\lambda}^{(k+1)})$ such that

$$A(\mathbf{u}^{(k+1)}) + \lambda_{\nu}^{(k+1)} \nu = \mathbf{f}, \quad (4.13)$$

$$u_{\nu,p}^{(k+1)} = 0 \quad \text{for all } p \in \mathcal{A}_{k+1}, \quad (4.14)$$

$$u_{\nu,p}^{(k+1)} = u_{\nu,p}^{(k)} + c\lambda_{\nu,p}^{(k+1)} \quad \text{for all } p \in \mathcal{I}_{k+1}. \quad (4.15)$$

- (iv) If $\|(\mathbf{u}^{(k+1)}, \boldsymbol{\lambda}^{(k+1)}) - (\mathbf{u}^{(k)}, \boldsymbol{\lambda}^{(k)})\| \leq \epsilon$, $\|\mathcal{R}(\mathbf{u}^{(k+1)}, \boldsymbol{\lambda}^{(k+1)})\| \leq \epsilon$ and $\mathcal{A}_{k+1} = \mathcal{A}_k$ then stop, else goto (ii).

Even if it was not referred to as an active set type method in [29], the algorithm fulfills the same objective than the active set strategy presented in Section 4.2, that is to say to find the correct subset \mathcal{A} of all nodes in contact with the perfectly rigid obstacle. However, the establishment of the subset $\mathcal{I} = \mathcal{S} \setminus \mathcal{A}$ changes according to the algorithm computed. In the primal dual active set method, the inactive set is obtained by using homogeneous Neumann boundary condition while, in the projection iterative method, the Robin condition $u_{\nu,p}^{(k+1)} = u_{\nu,p}^{(k)} + c\lambda_{\nu,p}^{(k+1)}$ for all $p \in \mathcal{I}_{k+1}$ is used instead. As a consequence, the non linear equation (4.13) can be solved by a linearized Newton method in which the Robin condition (4.15) has to be included beforehand. It leads to a differential of $\mathcal{R}\mathbf{u}(\mathbf{u}^{(k)}, \boldsymbol{\lambda}^{(k)})$ with respect to $\mathbf{u}^{(k)}$ different from the case of the primal dual active set method.

Remark 5. *We also insist on the fact that for the projection iterative method, it is not necessary to consider additional fictitious nodes in the initial mesh as for the augmented Lagrangian method. This particular trait represents one of the main advantages of the active set type methods.*

5. Convergence analysis of the projection iterative method

Since the convergence of active set type methods remains a challenging and open problem in the framework of hyperelasticity, in this section we investigate the convergence of the projection iterative algorithm in the infinitesimal strain theory. Therefore, under the hypothesis of small displacement-gradient theory, the first Piola-Kirchhoff tensor $\mathbf{\Pi}$ can be replaced by the Cauchy stress tensor $\boldsymbol{\sigma}$, since $\|\mathbf{u}\| \ll 1$ and $\|\nabla \mathbf{u}\| \ll 1$ (cf [8, p. 71]). In this part only, additional notations compatible with the small strain theory are introduced. We denote by \mathbb{S}^d the space of second order symmetric tensor on \mathbb{R}^d and we consider the space Q defined by

$$Q = \{\boldsymbol{\sigma} = (\sigma_{ij}) : \sigma_{ij} = \sigma_{ji} \in L^2(\Omega)\}.$$

Note that $\boldsymbol{\varepsilon}$ represents the linearized strain tensor in the small displacement-gradient theory

$$\boldsymbol{\varepsilon}(\mathbf{v}) = (\varepsilon_{ij}(\mathbf{v})), \quad \varepsilon_{ij}(\mathbf{v}) = \frac{1}{2}(v_{i,j} + v_{j,i}).$$

Then, we can consider an elastic constitutive law given by the following relation

$$\boldsymbol{\sigma} = \mathcal{E}\boldsymbol{\varepsilon}(\mathbf{u}). \quad (5.1)$$

We also assume that the elasticity tensor \mathcal{E} satisfies the following conditions.

$$\left\{ \begin{array}{l} \text{(a) } \mathcal{E} : \Omega \times \mathbb{S}^d \rightarrow \mathbb{S}^d. \\ \text{(b) There exists } L_{\mathcal{E}} > 0 \text{ such that} \\ \quad \|\mathcal{E}(\mathbf{x}, \boldsymbol{\varepsilon}_1) - \mathcal{E}(\mathbf{x}, \boldsymbol{\varepsilon}_2)\| \leq L_{\mathcal{E}} \|\boldsymbol{\varepsilon}_1 - \boldsymbol{\varepsilon}_2\| \quad \forall \boldsymbol{\varepsilon}_1, \boldsymbol{\varepsilon}_2 \in \mathbb{S}^d, \text{ a.e. } \mathbf{x} \in \Omega. \\ \text{(c) There exists } m_{\mathcal{E}} > 0 \text{ such that} \\ \quad (\mathcal{E}(\mathbf{x}, \boldsymbol{\varepsilon}_1) - \mathcal{E}(\mathbf{x}, \boldsymbol{\varepsilon}_2)) \cdot (\boldsymbol{\varepsilon}_1 - \boldsymbol{\varepsilon}_2) \geq m_{\mathcal{E}} \|\boldsymbol{\varepsilon}_1 - \boldsymbol{\varepsilon}_2\|^2 \\ \quad \forall \boldsymbol{\varepsilon}_1, \boldsymbol{\varepsilon}_2 \in \mathbb{S}^d, \text{ a.e. } \mathbf{x} \in \Omega. \\ \text{(d) The mapping } \mathbf{x} \mapsto \mathcal{E}(\mathbf{x}, \boldsymbol{\varepsilon}) \text{ is measurable on } \Omega, \text{ for any } \boldsymbol{\varepsilon} \in \mathbb{S}^d. \\ \text{(e) The mapping } \mathbf{x} \mapsto \mathcal{E}(\mathbf{x}, \mathbf{0}_{\mathbb{S}^d}) \text{ belongs to } Q. \end{array} \right. \quad (5.2)$$

Remark 6. Note that the previous hypotheses were used in [27, p. 126] to prove the uniqueness of the weak solution.

Let (\cdot, \cdot) denote the extension of the usual $L^2(\Gamma)$ scalar product to $H^{1/2}(\Gamma) \times H^{-1/2}(\Gamma)$. In order to establish the convergence analysis of the projection iterative method for the case of small strain theory, we have to consider and to prove preliminary results presented in the form of two lemmas.

Lemma 5.1. Denote by $(\mathbf{u}, \boldsymbol{\sigma})$ the solution of the Signorini problem \mathcal{P} , and $(\mathbf{u}^{(k+1)}, \boldsymbol{\sigma}^{(k+1)})$ the solution obtained at the iteration $k+1$ of the projection iterative method we have

$$(\sigma_{\nu}^{(k+1)}, u_{\nu}^{(k)} - u_{\nu})_{\Gamma_3} \geq (\sigma_{\nu}^{(k+1)}, u_{\nu}^{(k)} - u_{\nu}^{(k+1)})_{\Gamma_3}. \quad (5.3)$$

Proof. With the complementary condition (2.3), we have

$$(\sigma_{\nu}, u_{\nu}^{(k+1)} - u_{\nu})_{\Gamma_3} = (\sigma_{\nu}, u_{\nu}^{(k+1)})_{\Gamma_3}.$$

Also, since

$$u_{\nu}^{(k+1)} = -[-u_{\nu}^{(k)} + c\sigma_{\nu}^{(k+1)}]_{+} \leq 0 \text{ and } \sigma_{\nu} \leq 0,$$

we obtain that

$$(\sigma_{\nu}, u_{\nu}^{(k+1)} - u_{\nu})_{\Gamma_3} \geq 0. \quad (5.4)$$

Applying now the Green formula, we have:

$$\begin{aligned} \int_{\Omega} (\boldsymbol{\sigma}^{(k+1)} - \boldsymbol{\sigma}) \cdot (\boldsymbol{\varepsilon}(\mathbf{u}^{(k+1)}) - \boldsymbol{\varepsilon}(\mathbf{u})) \, dx &= \int_{\Gamma} (\boldsymbol{\sigma}^{(k+1)} - \boldsymbol{\sigma}) \boldsymbol{\nu} \cdot (\mathbf{u}^{(k+1)} - \mathbf{u}) \, da \\ &\quad - \int_{\Omega} \text{Div}(\boldsymbol{\sigma}^{(k+1)} - \boldsymbol{\sigma}) \cdot (\mathbf{u}^{(k+1)} - \mathbf{u}) \, dx. \end{aligned}$$

By using (2.6), (2.7), (2.8) and (2.10) we obtain

$$\int_{\Omega} (\boldsymbol{\sigma}^{(k+1)} - \boldsymbol{\sigma}) \cdot (\boldsymbol{\varepsilon}(\mathbf{u}^{(k+1)}) - \boldsymbol{\varepsilon}(\mathbf{u})) \, dx = (\sigma_{\nu}^{(k+1)} - \sigma_{\nu}, u_{\nu}^{(k+1)} - u_{\nu})_{\Gamma_3}, \quad (5.5)$$

besides, with (5.2)(c) and (5.1)

$$\int_{\Omega} (\boldsymbol{\sigma}^{(k+1)} - \boldsymbol{\sigma}) \cdot (\boldsymbol{\varepsilon}(\mathbf{u}^{(k+1)}) - \boldsymbol{\varepsilon}(\mathbf{u})) \, dx \geq m_{\mathcal{E}} \|\mathbf{u}^{(k+1)} - \mathbf{u}\|_{\mathbb{V}}^2 \geq 0, \quad (5.6)$$

and, by combining (5.5) and (5.6),

$$(\sigma_{\nu}^{(k+1)} - \sigma_{\nu}, u_{\nu}^{(k+1)} - u_{\nu})_{\Gamma_3} \geq 0. \quad (5.7)$$

Then, according to (5.4) and (5.7)

$$(\sigma_{\nu}^{(k+1)}, u_{\nu}^{(k+1)} - u_{\nu})_{\Gamma_3} \geq (\sigma_{\nu}, u_{\nu}^{(k+1)} - u_{\nu})_{\Gamma_3} \geq 0.$$

From there, we deduce Lemma 5.1

$$\begin{aligned} (\sigma_\nu^{(k+1)}, u_\nu^{(k)} - u_\nu)_{\Gamma_3} &= (\sigma_\nu^{(k+1)}, u_\nu^{(k)} - u_\nu^{(k+1)} + u_\nu^{(k+1)} - u_\nu)_{\Gamma_3} \\ &\geq (\sigma_\nu^{(k+1)}, u_\nu^{(k)} - u_\nu^{(k+1)})_{\Gamma_3}. \end{aligned}$$

□

Lemma 5.2. Denote by $(\mathbf{u}, \boldsymbol{\sigma})$ the solution of the Signorini problem \mathcal{P} , and $(\mathbf{u}^{(k+1)}, \boldsymbol{\sigma}^{(k+1)})$ the solution obtained at the iteration $k+1$ of the projection iterative method; then

$$\|u_\nu^{(k+1)} - u_\nu\|_{\Gamma_3}^2 \leq \|u_\nu^{(k)} - c\sigma_\nu^{(k+1)} - u_\nu\|_{\Gamma_3}^2 - \|u_\nu^{(k+1)} + c\sigma_\nu^{(k+1)} - u_\nu^{(k)}\|_{\Gamma_3}^2. \quad (5.8)$$

Proof. Let us consider K , a nonempty closed convex subset, x , a vector of K , and $P_K(x)$, the projector of x on K . Therefore, we have the following proposition proved in [27, p. 13]

$$(P_K(x) - x, P_K(x) - y) \leq 0, \quad \forall y \in K.$$

Here, we consider

$$P_{\mathbb{R}^+}(-u_\nu^{(k)} + c\sigma_\nu^{(k+1)}) = [-u_\nu^{(k)} + c\sigma_\nu^{(k+1)}]_+ = -u_\nu^{(k+1)} \text{ and } y = -u_\nu \geq 0,$$

then we obtain

$$(u_\nu^{(k+1)} - (u_\nu^{(k)} - c\sigma_\nu^{(k+1)}), u_\nu^{(k+1)} - u_\nu)_{\Gamma_3} \leq 0, \quad (5.9)$$

so

$$\begin{aligned} \|u_\nu^{(k+1)} - u_\nu\|_{\Gamma_3}^2 &= \|u_\nu^{(k+1)} - (u_\nu^{(k)} - c\sigma_\nu^{(k+1)}) + (u_\nu^{(k)} - c\sigma_\nu^{(k+1)}) - u_\nu\|_{\Gamma_3}^2 \\ &= \|u_\nu^{(k+1)} - (u_\nu^{(k)} - c\sigma_\nu^{(k+1)})\|_{\Gamma_3}^2 + \|(u_\nu^{(k)} - c\sigma_\nu^{(k+1)}) - u_\nu\|_{\Gamma_3}^2 \\ &\quad + 2(u_\nu^{(k+1)} - (u_\nu^{(k)} - c\sigma_\nu^{(k+1)}), (u_\nu^{(k)} - c\sigma_\nu^{(k+1)}) - u_\nu)_{\Gamma_3} \\ &= \|(u_\nu^{(k)} - c\sigma_\nu^{(k+1)}) - u_\nu\|_{\Gamma_3}^2 - \|u_\nu^{(k+1)} - (u_\nu^{(k)} - c\sigma_\nu^{(k+1)})\|_{\Gamma_3}^2 \\ &\quad + 2(u_\nu^{(k+1)} - (u_\nu^{(k)} - c\sigma_\nu^{(k+1)}), u_\nu^{(k+1)} - u_\nu) \\ &\leq \|(u_\nu^{(k)} - c\sigma_\nu^{(k+1)}) - u_\nu\|_{\Gamma_3}^2 - \|u_\nu^{(k+1)} - (u_\nu^{(k)} - c\sigma_\nu^{(k+1)})\|_{\Gamma_3}^2. \end{aligned}$$

□

Using the above Lemmas, we can now prove the following theorem

Theorem 5.3. The sequence $\{u_\nu^{(k)}\}$, defined in Section 4.2 by the projection iterative method, converges to the unique solution u_ν of the Signorini problem as $k \rightarrow \infty$.

Proof. First, by using the Lemma 5.2, we have

$$\begin{aligned} \|u_\nu^{(k+1)} - u_\nu\|_{\Gamma_3}^2 &\leq \|u_\nu^{(k)} - c\sigma_\nu^{(k+1)} - u_\nu\|_{\Gamma_3}^2 \\ &\quad - \|u_\nu^{(k+1)} + c\sigma_\nu^{(k+1)} - u_\nu^{(k)}\|_{\Gamma_3}^2 \\ &\leq \|u_\nu^{(k)} - u_\nu\|_{\Gamma_3}^2 - \|u_\nu^{(k+1)} - u_\nu^{(k)}\|_{\Gamma_3}^2 \\ &\quad - 2(c\sigma_\nu^{(k+1)}, u_\nu^{(k)} - u_\nu) - 2(c\sigma_\nu^{(k+1)}, u_\nu^{(k+1)} - u_\nu^{(k)}), \end{aligned} \quad (5.10)$$

then, by the Lemma 5.1,

$$\|u_\nu^{(k+1)} - u_\nu\|_{\Gamma_3}^2 \leq \|u_\nu^{(k)} - u_\nu\|_{\Gamma_3}^2 - \|u_\nu^{(k+1)} - u_\nu^{(k)}\|_{\Gamma_3}^2. \quad (5.11)$$

Next, we consider $S = \sum_{k=0}^{\infty} \|u_{\nu}^{(k+1)} - u_{\nu}^{(k)}\|_{\Gamma_3}^2$

$$S \leq \sum_{k=0}^{\infty} (\|u_{\nu}^{(k)} - u_{\nu}\|_{\Gamma_3}^2 - \|u_{\nu}^{(k+1)} - u_{\nu}\|_{\Gamma_3}^2).$$

Since $\{u_{\nu}^{(k)}\}$ is bounded, with $u_{\nu}^{(\infty)} = \lim_{k \rightarrow \infty} u_{\nu}^{(k)}$, we deduce

$$S \leq \|u_{\nu}^{(0)} - u_{\nu}\|_{\Gamma_3}^2 - \|u_{\nu}^{(\infty)} - u_{\nu}\|_{\Gamma_3}^2 < \infty. \quad (5.12)$$

It means that the infinite sum of the terms of the sequence $\|u_{\nu}^{(k+1)} - u_{\nu}^{(k)}\|_{\Gamma_3}^2$ converges. We deduce that

$$\lim_{k \rightarrow \infty} \|u_{\nu}^{(k+1)} - u_{\nu}^{(k)}\|_{\Gamma_3}^2 = 0. \quad (5.13)$$

Therefore $\{u_{\nu}^{(k)}\}$ is a Cauchy sequence. Let the couple $(u^*, \sigma^*) = (u_{\nu}^{(\infty)}, \sigma_{\nu}^{(\infty)})$, with $u_{\nu}^{(\infty)} = \lim_{k \rightarrow \infty} u_{\nu}^{(k)}$ and $\sigma_{\nu}^{(\infty)} = \lim_{k \rightarrow \infty} \sigma_{\nu}^{(k)}$. Such a couple verifies the fixed point problem (4.9) that is the solution of the Signorini problem; therefore

$$u^* = u_{\nu} \text{ and } \sigma^* = \sigma_{\nu}, \quad (5.14)$$

which concludes the proof. \square

Note that the Theorem 2.1 does not provide a coercivity assumption, or at least a strong monotonicity assumption, for the Piola-Kirchhoff tensor Π , needed in (5.7). Therefore, whether Theorem 5.3 still holds in the case of large deformation framework remains, for now, an open question which deserves to be investigated in the future.

6. Numerical simulations

The aim of this section is to present several numerical simulations which illustrate, amongst other, the behavior of the numerical solutions of the two active set type methods described in Section 4 compared to the augmented Lagrangian method. Moreover, in order to conduct an objective comparison of methods, the linearized subproblems resulting from each method are solved by the same numerical algorithm, namely a conjugate gradient method with incomplete LU factorization preconditioning. We carried out the numerical simulations based on two static frictionless contact problems: the Hertz half-sphere contact problem and the compression of a hyperelastic ring against a rigid foundation.

Note that the different numerical methods have been implemented in a Fortran computer code which is based on a MODULAR Finite Element library (MODULEF) developed by INRIA (Institut National de Recherche en Informatique et en Automatique, Rocquencourt, France). For more details, we refer to <https://www.rocq.inria.fr/modulef/english.html>.

6.1. Hertz half-sphere contact problem

Generally, it is quite difficult to find analytical solutions for contact problems, because of their complexity, however there are several exceptions studied in the Hertz theory [14]. For this reason, we describe in what follows the compression of a linear elastic half ball against a foundation that is included in the Hertz theory. The physical setting is depicted in Figure 1. There, the following notations are used:

$$\begin{aligned} \Omega &= \{(x_1, x_2) \in \mathbb{R}^2 : x_1^2 + (x_2 - R)^2 \leq R^2, x_2 \leq R\}, \\ \Gamma_1 &= \{(x_1, x_2) \in \mathbb{R}^2 : x_1 = 0, x_2 = R\}, \\ \Gamma_2 &= \{(x_1, x_2) \in \mathbb{R}^2 : x_2 = R, -R \leq x_1 \leq R\}, \\ \Gamma_3 &= \{(x_1, x_2) \in \mathbb{R}^2 : x_1^2 + (x_2 - R)^2 = R^2, x_2 \leq R\}. \end{aligned}$$

The domain Ω represents the cross section of a three-dimensional deformable body subjected to the action of traction in such a way that a plane deformation hypothesis is assumed. The horizontal component of the displacement field vanishes on Γ_1 . Vertical traction of density \mathbf{f}_2 acts on the boundary Γ_2 . No body forces are assumed to act on the body during the process. The body is in contact without friction with an obstacle on the part Γ_3 of its boundary. For the discretization, we have control over a parameter $N_{\Gamma_3}^h$ that describes the number of nodes on Γ_3^h (the number of nodes on Γ_2^h is, therefore, chosen accordingly in order to obtain regular-enough elements). In the configuration $N_{\Gamma_3}^h = 256$ depicted in Figure 1, 30356 elastic finite elements were used and the total number of degrees of freedom is equal to 30810. We model the material's behavior with an elastic linear constitutive law in which the elasticity tensor \mathcal{E} satisfies

$$(\mathcal{E}\boldsymbol{\varepsilon})_{\alpha\beta} = \frac{E\kappa}{(1+\kappa)(1-2\kappa)}(\varepsilon_{11} + \varepsilon_{22})\delta_{\alpha\beta} + \frac{E}{1+\kappa}\varepsilon_{\alpha\beta}, \quad 1 \leq \alpha, \beta \leq 2.$$

Here E is the Young modulus, κ the Poisson ratio of the material and $\delta_{\alpha\beta}$ denotes the Kronecker symbol.

For the computation below the following data were used:

$$\begin{aligned} E &= 150N/m^2, & \kappa &= 0.3, \\ \mathbf{f}_0 &= (0, 0)N/m^2, & \mathbf{f}_2 &= (0, -2)N/m \quad \text{on } \Gamma_2, \\ R &= 8m, & \text{stopping criterion} &: \epsilon = 10^{-5}. \end{aligned}$$

In Figure 2, the deformed configuration as well as the normal contact stresses on the boundary Γ_3 are plotted.

Accuracy of the methods comparing to the analytical solution. According to the Hertz theory, it is possible to calculate the analytical solution given by the following normal pressure distribution on Γ_3 :

$$\begin{cases} if & |x_1| < b, & p_\nu = -\frac{4R\mathbf{f}_{2y}}{\pi b^2}\sqrt{b^2 - x_1^2} & (contact), \\ else & p_\nu = 0 & (no contact), \end{cases} \quad (6.1)$$

with $b = 2\sqrt{\frac{2R^2\mathbf{f}_{2y}(1-\kappa^2)}{E\pi}}$. We present now the comparison between the numerical solutions, obtained by the projection iterative method, the primal dual active set method, the augmented Lagrangian method, and the analytical solution (6.1), given by the Hertz theory.

In Figure 3, we investigate the accuracy of the methods on Γ_3 by plotting the normal contact stress σ_ν with respect to the abscissa for each method. We note that the analytical solution and the numerical solutions are already almost indistinguishable. Therefore, as expected, the projection iterative method and the primal dual active set method are reliable on this test case. In Figure 4, the difference ($\Delta_{Analytic}$) between the analytical solution and the normal contact stress σ_ν obtained with the 3 numerical methods are also plotted. Note that, while there is a very slight difference between the projection iterative method and the augmented Lagrangian method, no difference is visible at first sight between the primal dual active set method and the augmented Lagrangian method.

Performances of the algorithms. In Table 1, we give the number of iterations for the convergence of the projection iterative method and the augmented Lagrangian method with respect to the arbitrary positive parameter c used in Section 4.2 and with respect to the number of nodes of Γ_3^h , $N_{\Gamma_3}^h$. In Table 2, we conduct the same study for the primal dual active set method with respect to the arbitrary positive parameter γ used in Section 4.1.

According to Tables 1–2, as expected, the arbitrary positive parameters c and γ do not have a significant effect on the number of iterations for the projection iterative method and the primal dual

active set method. However, such statements are not exactly verified for the projection iterative method in the cases where c is less than or equal to 10. This is due to the fact that the condition (4.15) tends to the condition (4.8) when c tends to infinity. Furthermore, the number of iterations to reach the convergence is identical for the primal dual active set method and the augmented Lagrangian method, and a such trait comes from that the second equation of (4.2) corresponds exactly to the second equation of (3.10). Besides, note that the number of iterations for the augmented Lagrangian method and the two active set type methods is not degraded with the increasing of $N_{\Gamma_3}^h$.

Next, in Figure 5–7 we provide the evolution of the error $E_k = \|\mathbf{x}^{(k)} - \mathbf{x}^{(k-1)}\|_2$ with respect to the iteration index k for each method, with $c = \gamma = 10^4$, and for 3 values of $N_{\Gamma_3}^h$ ($N_{\Gamma_3}^h = 128, 256, 512$). There is almost no difference between the curve obtained with the projection iterative method and the curve obtained with primal dual active set. Also it seems that both methods have an error evolution similar to that of the augmented Lagrangian method.

In Table 3, we provide the CPU time of the simulation for each method with respect to $N_{\Gamma_3}^h$. The two active set type methods are faster by far, in term of CPU time, than the augmented Lagrangian method. This behavior can be explained by the use of the Lagrange multipliers for the augmented Lagrangian method which worsen the condition number of the linearized systems coming from the Newton method and therefore this leads to an increase of the solution’s CPU time of the linearized systems. Such a result must be highlighted by the actual size of the tangent linear system, i.e. the number of degrees of freedom, in both cases with respect to the discretization considered:

- $N_{\Gamma_3}^h = 128$: 7921 dof for the augmented Lagrangian method compared to 7792 dof for the active set type methods,
- $N_{\Gamma_3}^h = 256$: 31067 dof for the augmented Lagrangian method compared to 30810 dof for the active set type methods,
- $N_{\Gamma_3}^h = 512$: 123065 dof for the augmented Lagrangian method compared to 122552 dof for the active set type methods.

Note that, as already implied in the presentation of the algorithms, the tangent linear system arising from the active set type methods is smaller since we do not use the Lagrange multiplier in those cases. In fact, given the small differences between the primal dual active set method and the projection iterative method, we can consider that they are equally fast, both in term of iteration and in term of CPU time.

Evolution of the deformed meshes during the iterative process. We display now in Figures 8–9 the deformed meshes at different steps of convergence of the active set methods and the augmented Lagrangian method. More precisely, the deformed configurations are plotted for the iteration number 1, 3, 5 and 8. It is relevant to compare them since the three methods converge with the same number of iterations for $c = \gamma = 10^4$. Unexpectedly, the deformed meshes during the iterative process of the augmented Lagrangian method and the active set type methods are identical to the point that they are stackable. This behavior can be explained by the fact that the contact conditions (4.1) and (4.9) used for the two active set methods correspond exactly to the second equation of the non linear system (3.10) arising from the augmented Lagrangian method.

Error estimates. At last, we provide and check the numerical convergence order of the active set methods. In order to do that, a sequence of numerical solutions is computed by using triangulations of the body according to the spatial discretization parameter h . Since the solutions are virtually identical, we provide this numerical study for the projection iterative method. The numerical estimated error values $\|\mathbf{u} - \mathbf{u}^h\|_V$, denoted by E^h in Figure 10, are computed for several discretization parameters of h . Here, the boundary Γ_3 of Ω is divided into $1/h$ equal parts. The numerical solution corresponding to $h = 1/512$ is taken as the “exact” solution, which is used to compute the errors of the numerical solutions with 6 higher values of h . Therefore, the results obtained for the following values of h : $h = 1/64$, $h = 1/96$, $h = 1/128$, $h = 1/192$, $h = 1/256$ and $h = 1/384$ are plotted. The

numerical results are presented in Figure 10 where the dependence of the error estimate $\|\mathbf{u} - \mathbf{u}^h\|_V$ with respect to h is plotted. According to Figure 10, the curve of the numerical error estimates is asymptotically linear with respect to h , which is consistent with the theoretical error estimates established in [5, 20] for the case of the small deformation theory.

6.2. Compression of a hyperelastic ring against a foundation

In this section, we consider a second representative application in order to assess the performances of the active set type methods in the case of large deformation framework. It concerns an academic frictionless contact problem based on the compression of a hyperelastic ring against a rigid foundation. Details on the physical setting of the problem, depicted in Figure 11, are given below:

$$\begin{aligned}\Omega &= \{(x_1, x_2) \in \mathbb{R}^2 : R_i^2 \leq x_1^2 + (x_2 - R_e)^2 \leq R_e^2\}, \\ \Gamma_1 &= \widehat{AB}, \quad \Gamma_2 = \emptyset, \\ \Gamma_3 &= \{(x_1, x_2) \in \mathbb{R}^2 : x_1^2 + (x_2 - R_e)^2 = R_e^2, \quad x_2 \leq \sqrt{2}R_e\}.\end{aligned}$$

The domain Ω represents the cross section of a three-dimensional hyperelastic body subjected to the action of displacement in such a way that the plane stress hypothesis is assumed. The foundation is given by $\{(x_1, x_2) \in \mathbb{R}^2 : x_2 \leq 0\}$. On the part Γ_1 , a vertical displacement \mathbf{u}_0 is imposed. No forces are assumed to act on the hyperelastic body during the process. The body is in frictionless contact with an obstacle on the part Γ_3 of the boundary. For the discretization, we have control over a parameter N_Γ^h that describes the number of nodes on Γ (the number of nodes on the thickness of the ring is, therefore, chosen accordingly in order to obtain regular-enough elements). In the configuration $N_\Gamma^h = 256$ depicted in Figure 11, the boundary Γ_3 is divided in 192 equal parts, 6144 hyperelastic finite elements were used for a total number of degrees of freedom equal to 6656. The compressible material response, considered here, is governed by a variant of the Ogden constitutive law (see [9]) defined by the following energy density

$$W(\mathbf{C}) = c_1(I_1 - 3) + c_2(I_2 - 3) + a(I_3 - 1) - (c_1 + 2c_2 + a) \ln I_3.$$

Here I_1, I_2 and I_3 represent the three invariants of the tensor \mathbf{C} , with $\mathbf{C} = \mathbf{F}^T \mathbf{F}$. For the numerical experiments, the data are:

$$\begin{aligned}\mathbf{u}_0 &= (0, -14)m, \\ \mathbf{f}_0 &= (0, 0)N/m^2, \quad \mathbf{f}_2 = \begin{cases} (0, 0)N/m & , \\ (0, 0)N/m & , \end{cases} \\ c_1 &= 0.5MPa, \quad c_2 = 0.5 \times 10^{-2}MPa, \quad a = 0.35MPa, \\ R_i &= 9m, \quad R_e = 10m.\end{aligned}$$

In Figure 12, the deformed configuration as well as the normal contact stresses on the contact boundary Γ_3 are plotted.

As in the previous Section 6.1, we present the comparison between the numerical solutions obtained by the active set type methods and the augmented Lagrangian method with respect to the numerical accuracy, convergence and performances of the methods.

First in Figure 13, we plot the normal contact stress Π_ν with respect to the abscissa on Γ_3 for the three mentioned methods. It is clear that the methods do not present any significant differences, which leads us to say that the active set type methods are accurate even in the large deformation framework on this numerical test compared to the augmented Lagrangian methods.

Now, in Tables 4–5, we study the evolution of the number of iterations needed for the convergence of both the projection iterative method and the primal dual active set method compared to the

augmented Lagrangian method. In the case of this hyperelastic contact example, the number of iterations is more dependent to the value of c than in the case of the Hertz contact problem of Section 6.1. We remark that, when $c \leq 10$, the algorithm even fails to converge (Ncv). However, according to Tables 4 and 5, for a large value of c , greater or equal to 10^4 , the number of iterations needed for the convergence of the projection iterative method becomes constant and, is substantially equal to that obtained for the convergence of the primal dual active set method. Furthermore, we remark that the values of γ hardly impact the number of iterations for the primal dual active set method. Moreover, unlike the numerical example studied in Section 6.1, both the primal dual active set method and the projection iterative method take extra iterations to converge, compared to the augmented Lagrangian method.

Next, we provide in Figures 14–16 the evolution of $E_k = \|\mathbf{x}^{(k)} - \mathbf{x}^{(k-1)}\|_2$ with respect to the iteration index k for the augmented Lagrangian method and the active set methods for several values of discretization ($N_\Gamma^h = 128, 256, 512$). Although the projection iterative method requires some extra iterations to converge, it can be seen that the convergence of the projection iterative method is smoother than the convergence of the primal dual active set method.

At last, we provide in Table 6 a comparison of the methods in term of CPU time to reach the convergence with respect to the size of the problem. It leads us to say that the two active set type methods have a faster convergence in term of CPU time than the augmented Lagrangian method. This behavior is due to the fact that the two active set methods do not use any Lagrange multipliers. As for the first numerical example (section 6.1), such a result must be highlighted by the actual size of the tangent linear system, i.e. the number of degrees of freedom, in both cases with respect to the discretization considered:

- $N_\Gamma^h = 128$: 1889 dof for the augmented Lagrangian method compared to 1792 dof for the active set type methods,
- $N_\Gamma^h = 256$: 6849 dof for the augmented Lagrangian method compared to 6656 dof for the active set type methods,
- $N_\Gamma^h = 512$: 25985 dof for the augmented Lagrangian method compared to 25600 dof for the active set type methods.

This is why the avoidance of the Lagrange multipliers remains a solid argument to rather choose the active set type methods over the augmented Lagrangian method.

7. Conclusion

This paper provides the analysis of two active set type methods through a classical problem from the contact mechanics literature, that is to say the Signorini problem both in the case of the large and small deformation. First, a variational formulation is derived from the mechanical problem and an existence result based on stored energy function properties is provided in the framework of hyperelasticity. Then, we derived a numerical approximation of the problem and provided a minimization formulation through the augmented Lagrangian formalism. After that, we presented two active set type methods with their algorithms. Next, we investigated the convergence of the projective iterative algorithm in the infinitesimal strain theory; the proof is based on considerations about projection operators and the properties of the elasticity operator. Note that the same properties were used for the uniqueness of the weak solution in the small deformation theory. Then, we presented several numerical simulations in order to compare the behavior of the two active set type methods. We carried them out on two test problems, with the augmented Lagrangian method taken as a reference: one in the small deformation framework with the Hertzian contact and one in the large deformation framework with the compression of a hyperelastic ring against a rigid foundation. While the results showed quite clearly that the active set type methods are effective on the first

test case, both in term of convergence rate and in term of CPU time, the second test case must be studied with caution. Indeed, these active set methods took more iterations than the augmented Lagrangian to converge. However, both of them were faster in term of CPU time than the augmented Lagrangian. Nevertheless, as already said, the fact that the active set type methods does not require the use of the Lagrange multipliers cannot be neglected from an implementation point of view. Therefore, for all these reasons, it seems consistent to consider an active set type method over the augmented Lagrangian method.

At this point, we can already highlight some prospects which could be considered in the continuation of this paper. From a theoretical point of view, we showed the convergence of the projection iterative algorithm in the small deformation framework, using only the hypotheses needed for the uniqueness of the weak solution in the same framework. Since we presented an existence result in the large deformation framework based on several different hypotheses, a challenging prospect would be to prove the convergence of this algorithm in this difficult case and this point remains for now an open question, at the best of our knowledge. Besides, we only studied frictionless static contact problem. It could be interesting to consider the challenging case of a frictional contact problem or the dynamic case.

References

- [1] P. Alart and A. Curnier, A mixed formulation for frictional contact problems prone to Newton like solution methods, *Comput. Meth. Appl. Mech., Engrg.* **92**, 1991, 353-375.
- [2] Y. Ayyad and M. Barboteu, Formulation and analysis of two energy-consistent methods for nonlinear elastodynamic frictional contact problems, *Journal of Computational and Applied Mathematics* **228**, 2009, 254–269.
- [3] M. Barboteu, D. Danan, and M. Sofonea, *A Hyperelastic Dynamic Frictional Contact Model with Energy-Consistent Properties*, Springer International Publishing Switzerland W. Han et al. (eds.), *Advances in Variational and Hemivariational Inequalities with Applications, Advances in Mechanics and Mathematics* **33**, DOI 10.1007/978-3-319-14490-0 10, 2015.
- [4] F. Ben Belgacem, P. Hild and P. Laborde, *Extension of the mortar finite element method to a variational inequality modeling unilateral contact*, *Mathematical Models and Methods in Applied Sciences*, **9**, 1999, 287-303.
- [5] F. Ben Belgacem and Y. Renard, *Hybrid finite element methods for the Signorini problem*, *Mathematics of Computation*, **72**(243), 2003, 1117-1145.
- [6] P. Boieri, F. Gastaldi, and D. Kinderlehrer, Existence, Uniqueness, and Regularity Results for the Two-Body Contact Problem. *Applied Mathematics and Optimization*, **15**, 1987, 251-277.
- [7] F. Chouly, P. Hild and Y. Renard. A Nitsche finite element method for dynamic contact : 1. Semi-discrete problem analysis and time-marching schemes. 2014.
- [8] P.G. Ciarlet, *Mathematical Elasticity, Vol. I : Three-Dimensional Elasticity*, Series Studies in Mathematics and its Applications, North-Holland, Amsterdam, 1988.
- [9] P.G. Ciarlet and G. Geymonat, Sur les lois de comportement en élasticité non-linéaire compressible, *C. R. Acad. Sci.*, **295**(I), 1982, 423–426.
- [10] C. Eck, J. Jarušek and M. Krbeč, *Unilateral Contact Problems: Variational Methods and Existence Theorems*, Pure and Applied Mathematics **270**, Chapman/CRC Press, New York, 2005.
- [11] W. Han and M. Sofonea, *Quasistatic Contact Problems in Viscoelasticity and Viscoplasticity*, Studies in Advanced Mathematics **30**, American Mathematical Society–International Press, 2002.

- [12] J. Haslinger and I. Hlaváček, *Numerical Methods for Unilateral Problems in Solid Mechanics*, in Handbook of Numerical Analysis, J.-L. Lions and P. Ciarlet, eds., Vol IV, North-Holland, Amsterdam, 1996, 313–485.
- [13] J. Haslinger, I. Hlaváček and J. Nečas, *Contact between two elastic bodies - I. continuous problems*, in Aplikace Matematiky, **25**, 1980, 324-347.
- [14] H. Hertz, Über die Berührung fester elastischer Körper, Journal für reine und angewandte Mathematik, **92**, 1881, p156-171.
- [15] M. Hintermuller, K. Ito, and K. Kunish. *The primal dual active set strategy as a semismooth Newton Method*, SIAM J Optim, **13**, 2002, 865-888.
- [16] M. Hintermuller, V. Kovtunenکو, and K. Kunish. *Semismooth Newton methods for a class of unilaterally constrained variational problems*, Adv. In Math. Sci. and Appl. **147**, 2004, 513-535.
- [17] I. Hlaváček, J. Haslinger, J. Nečas and J. Lovíšek, *Solution of Variational Inequalities in Mechanics*, Springer-Verlag, New York, 1988.
- [18] S. Hueber and B.I. Wohlmuth, *A primal dual active set strategy for non-linear multibody contact problems*, Computer Methods in Applied Mechanics and Engineering, **194**, Issues 27-29, 22 July 2005, 3147-3166.
- [19] H.B. Khenous, J. Pommier, and Y. Renard, Hybrid discretization of the Signorini problem with Coulomb friction. Theoretical aspects and comparison of some numerical solvers, *Applied Numerical Mathematics* **56**, 2006, 163–192.
- [20] N. Kikuchi and J.T. Oden, *Contact Problems in Elasticity: A Study of Variational Inequalities and Finite Element Methods*, SIAM, Philadelphia, 1988.
- [21] T. Laursen, *Computational Contact and Impact Mechanics*, Springer, Berlin, 2002.
- [22] P. Le Tallec, *Numerical Methods for Nonlinear Three-dimensional Elasticity*, in Handbook of Numerical Analysis, Vol. III, (P. G. Ciarlet and J. L. Lions eds.) North-Holland, 1994
- [23] J.J. Moreau, *Application of convex analysis to some problems of dry friction*, Trends of Pure Mathematics Applied to Mechanics, Zorski ed., 1979.
- [24] P.D. Panagiotopoulos, *Inequality Problems in Mechanics and Applications*, Birkhäuser, Boston, 1985.
- [25] M. Shillor, M. Sofonea, and J. Telega, *Models and Variational Analysis of Quasistatic Contact*, Lecture Notes in Physics **655**, Springer, Berlin Heidelberg, 2004.
- [26] A. Signorini, *Sopra alcune questioni di elastostatica*, Atti della Società Italiana per il Progresso delle Scienze, 1933.
- [27] M. Sofonea and A. Matei, *Mathematical Models in Contact Mechanics*, London Mathematical Society Lecture Note Series **398**, Cambridge University Press, Cambridge, 2012.
- [28] P. Wriggers, *Computational Contact Mechanics*, Wiley, Chichester, 2002.
- [29] S. Zhang, J. Zhu, A projection iterative algorithm boundary element method for the Signorini Problem, *Engineering Analysis with Boundary Elements*, **37**, 2013, 176-181.

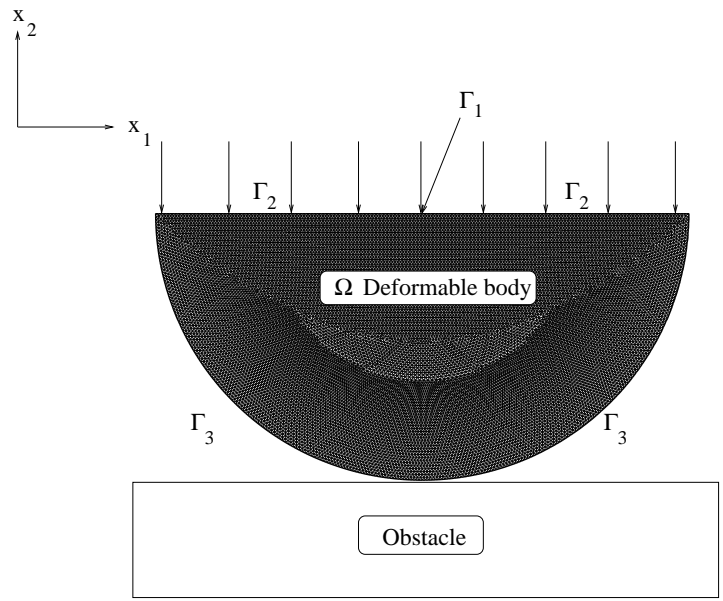


Figure 1: Physical setting of the Hertz contact problem.

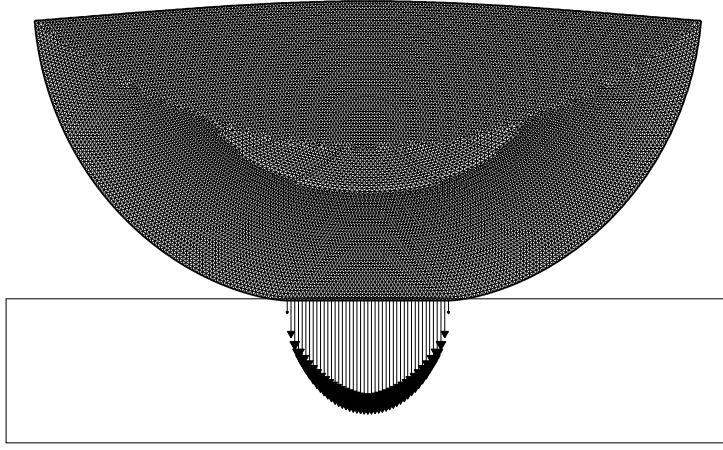


Figure 2: Deformed mesh and normal contact stresses on Γ_3 .

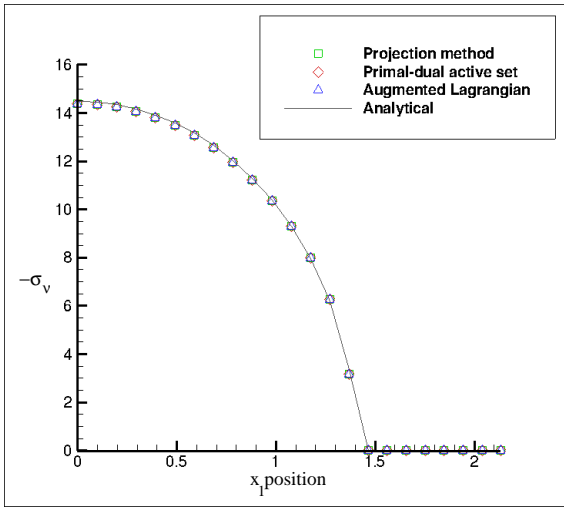


Figure 3: Normal contact stress σ_ν on Γ_3 .

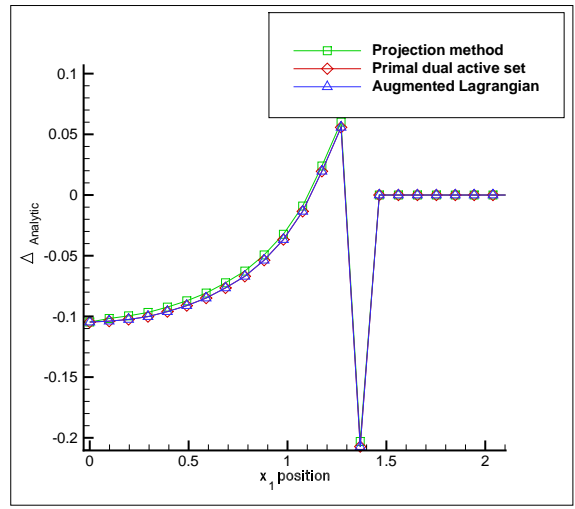


Figure 4: Evolution of $\Delta_{Analytic}$ for the three methods with respect to the abscissa ($c = \gamma = 10^4$).

$N_{\Gamma_3}^h$	Projection iterative method					Augm. Lagrangian
	$c = 1$	$c = 10$	$c = 10^2$	$c = 10^3$	$c = 10^4$	
128	11	8	7	7	7	7
256	11	9	8	8	8	8
512	18	10	9	9	9	9

Table 1: Number of iterations for the convergence of the projection iterative method with respect to c and $N_{\Gamma_3}^h$.

$N_{\Gamma_3}^h$	Primal dual active set method					Augm. Lagrangian
	$\gamma = 1$	$\gamma = 10$	$\gamma = 10^2$	$\gamma = 10^3$	$\gamma = 10^4$	
128	7	7	7	7	7	7
256	8	8	8	8	8	8
512	9	9	9	9	9	9

Table 2: Number of iterations for the convergence of the primal dual active set method with respect to γ and $N_{\Gamma_3}^h$.

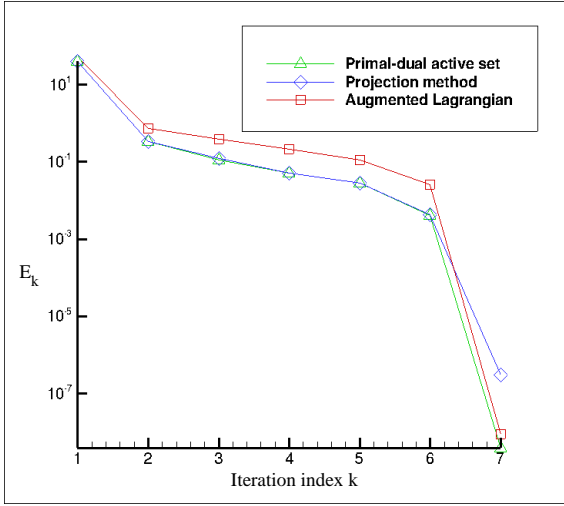


Figure 5: Evolution of E_k with respect to k for $N_{\Gamma_3}^h = 128$ ($c = \gamma = 10^4$).

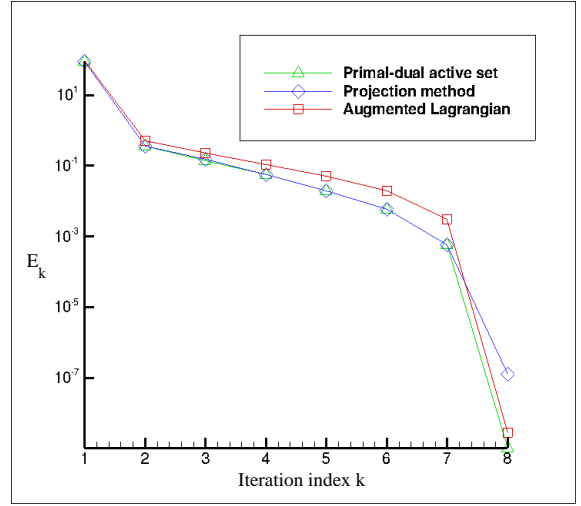


Figure 6: Evolution of E_k with respect to k for $N_{\Gamma_3}^h = 256$ ($c = \gamma = 10^4$).

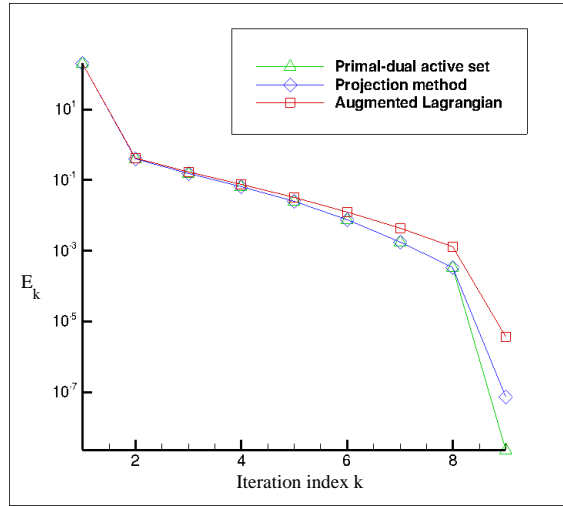


Figure 7: Evolution of E_k with respect to k for $N_{\Gamma_3}^h = 512$ ($c = \gamma = 10^4$).

$N_{\Gamma_3}^h$	Projection iterative	Primal dual active set	Augm. Lagrangian
128	5	4	7
256	29	29	54
512	208	205	472

Table 3: CPU time (in seconds) for each method with respect to $N_{\Gamma_3}^h$ with $c = 10^4$ and $\gamma = 10^4$.

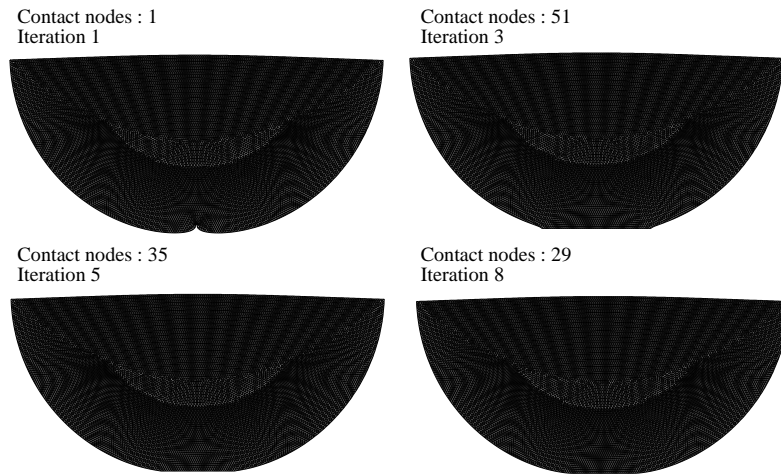


Figure 8: Deformed meshes during the iterative process of the augmented Lagrangian method with $N_{\Gamma_3}^h = 256$.

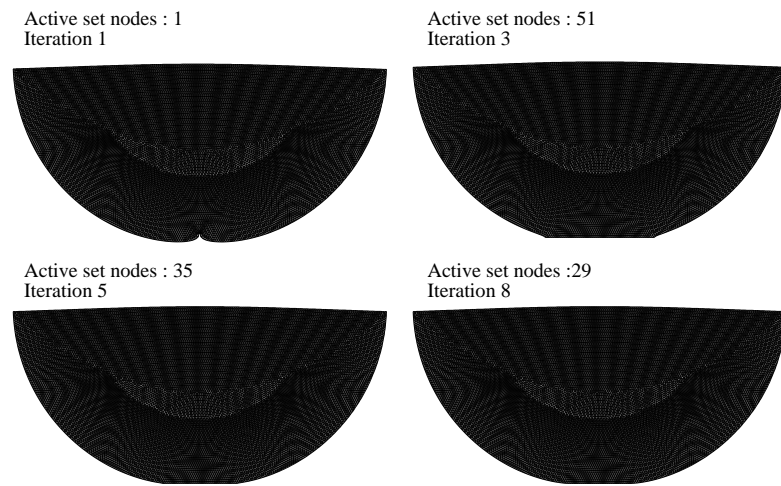


Figure 9: Deformed meshes during the iterative process for the primal dual active set method/the projection iterative method with $N_{\Gamma_3}^h = 256$.

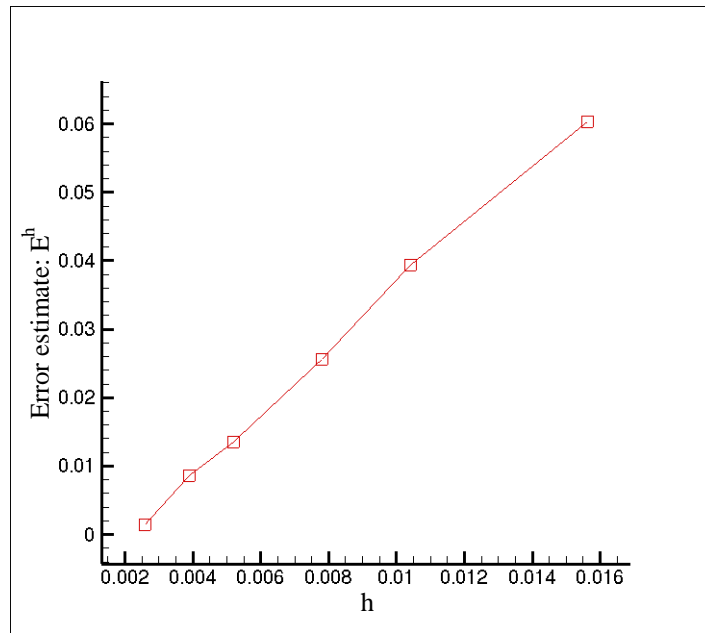


Figure 10: Estimated numerical errors.

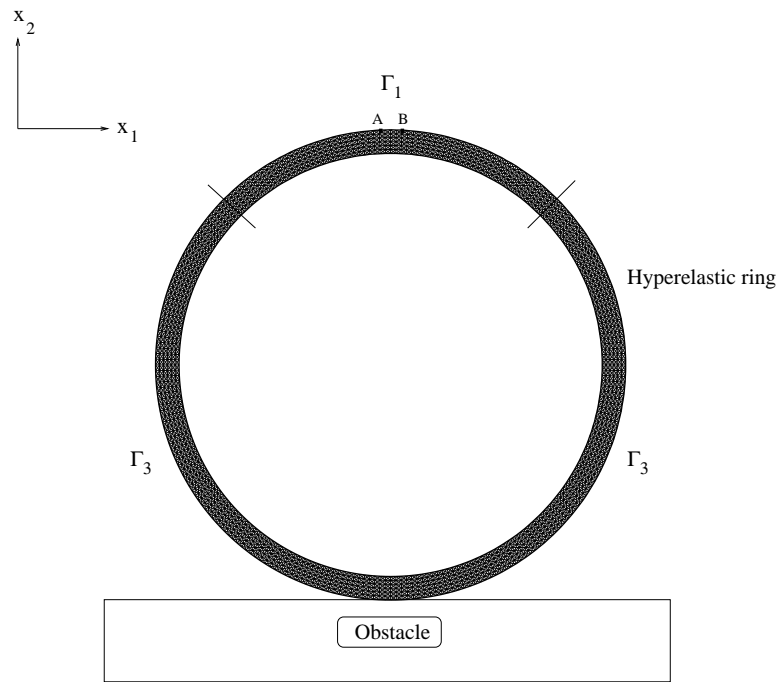


Figure 11: Physical setting of the hyperelastic contact problem.

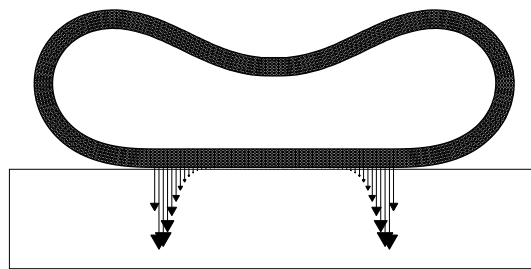


Figure 12: Deformed mesh with normal contact stresses on Γ_3 .

	Projection iterative method						Augm. Lagrangian
N_{Γ}^h	$c = 10$	$c = 10^2$	$c = 10^3$	$c = 10^4$	$c = 10^5$	$c = 10^6$	
128	Ncv	294	41	12	13	13	8
256	Ncv	171	45	14	19	16	9
512	Ncv	378	45	14	14	19	10

Table 4: Number of iterations for the convergence of the projection iterative method with respect to c and N_{Γ}^h .

	Primal dual active set method						Augm. Lagrangian
N_{Γ}^h	$\gamma = 10$	$\gamma = 10^2$	$\gamma = 10^3$	$\gamma = 10^4$	$\gamma = 10^5$	$\gamma = 10^6$	
128	12	12	12	12	12	12	8
256	13	13	13	13	15	14	9
512	14	14	14	14	14	14	10

Table 5: Number of iterations for the convergence of the primal dual active set method with respect to γ and N_{Γ}^h .

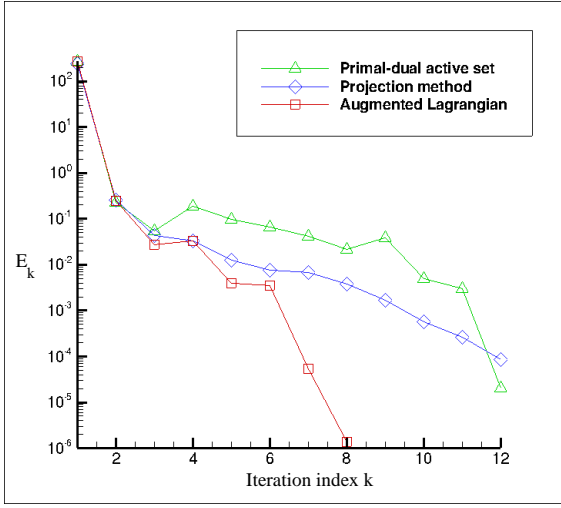


Figure 14: Evolution of E_k with respect to k for $N_\Gamma^h = 128$ ($c = \gamma = 10^4$).

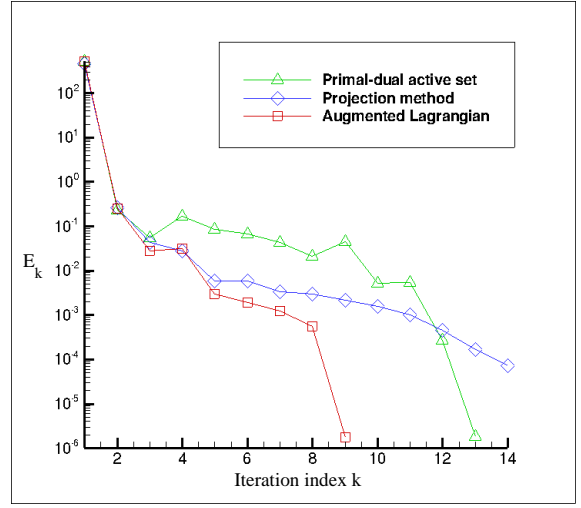


Figure 15: Evolution of E_k with respect to k for $N_\Gamma^h = 256$ ($c = \gamma = 10^4$).

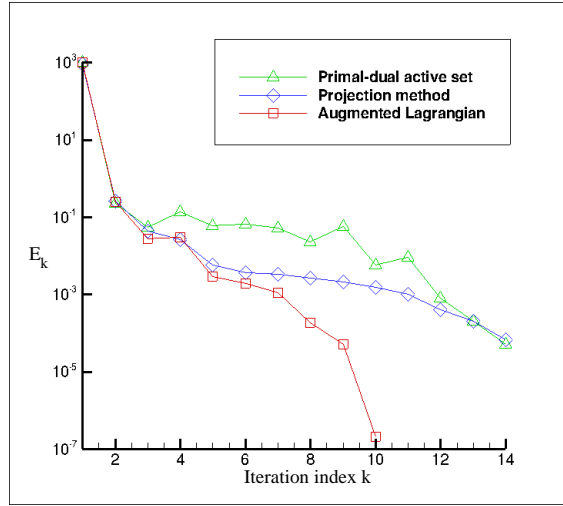


Figure 16: Evolution of E_k with respect to k for $N_\Gamma^h = 512$ ($c = \gamma = 10^4$).

N_{Γ}^h	Projection iterative	Primal dual active set	Augm. Lagrangian
128	1	1	1
256	19	17	43
512	89	87	160

Table 6: CPU time (in seconds) for each method with respect to N_{Γ}^h with $c = 10^4$ and $\gamma = 10^4$.